Latency Study and System Design Guidelines for Cooperative LTE-DSRC Vehicle-to-Everything (V2X) Communications including Smart Antenna

Junsung Choi

Thesis submitted to the faculty of the Virginia Polytechnic Institute and State University in partial fulfillment of the requirements for the degree of

Master of Science
In
Electrical Engineering

Carl B. Dietrich
Jeffrey H. Reed
Vuk Marojevic

December 14, 2016
Blacksburg, VA

Keywords: DSRC, LTE, V2X, warning, linear array antenna

Latency Study and System Design Guidelines for Cooperative LTE-DSRC Vehicle-to-Everything (V2X) Communications including Smart Antenna

Junsung Choi

ABSTRACT

Vehicle-related communications are a key application to be enabled by Fifth Generation (5G) wireless systems. The communications enabled by the future Internet of Vehicles (IoV) that are connected to every wireless device are referred to as Vehicle-to-Everything (V2X) communications. A major application of V2X communication systems will be to provide emergency warnings. This thesis evaluates Long-Term Evolution (LTE) and Dedicated Short Range Communications (DSRC) in terms of service quality and latency, and provides guidelines for design of cooperative LTE-DSRC systems for V2X communications. An extensive simulation analysis shows that (1) the number of users in need of warning has an effect on latency, and more so for LTE than for DSRC, (2) the DSRC *priority* parameter has an impact on the latency, and (3) wider system bandwidths and smaller cell sizes reduce latency for LTE. The end-to-end latency of LTE can be as high as 1.3 s, whereas the DSRC latency is below 15 ms for up to 250 users.

Also, improving performance of systems is as much as important as studying about latency. One method to improving performance is using a better suitable antenna for physical communication. The mobility of vehicles results in a highly variable propagation channel that complicates communication. Use of a smart, steerable antenna can be one solution. The most commonly used antennas for vehicular communication are omnidirectional. Such antennas have consistent performance over all angles in the horizontal plane; however, rapidly steerable directional antennas should perform better in

a dynamic propagation environment. A linear array antenna can perform dynamical appropriate azimuth pattern by having different weights of each element. The later section includes (1) identifying beam pattern parameters based on locations of a vehicular transmitter and fixed receivers and (2) an approach to find weights of each element of linear array antenna. Through the simulations with our approach and realistic scenarios, the desired array pattern can be achieved and array element weights can be calculated for the desired beam pattern. Based on the simulation results, DSRC is preferred to use in the scenario which contains large number of users with setup of higher priority, and LTE is preferred to use with wider bandwidth and smaller cell size. Also, the approach to find the controllable array antenna can be developed to the actual implementation of hardware with USRP.

Latency Study and System Design Guidelines for Cooperative LTE-DSRC Vehicle-to-Everything (V2X) Communications including Smart Antenna

Junsung Choi

GENERAL AUDIENCE ABSTRACT

Vehicle-related communications are a key application to be enabled by Fifth Generation (5G) wireless systems, which will be the next generation of cellular communication standard. The communications enabled by the future Internet of Vehicles (IoV) that are connected to every wireless device are referred to as Vehicle-to-Everything (V2X) communications. A major application of V2X communication systems will be to provide emergency warnings. This thesis evaluates Long-Term Evolution (LTE) and Dedicated Short Range Communications (DSRC), the standard for vehicular communication, in terms of service quality and latency, which are the major component parameters for the warning applications, and provides guidelines for design of cooperative LTE-DSRC systems for V2X communications. An extensive simulation analysis shows that (1) the number of users in need of warning has an effect on latency, and more so for LTE than for DSRC, (2) one parameter of DSRC has an impact on the latency, and (3) wider system bandwidths and smaller cell sizes reduce latency for LTE. Also, improving performance of systems is as much as important as studying about latency. One method to improving performance is using a better suitable antenna for physical communication. The most commonly used antennas for vehicular communication are omnidirectional antenna, which have consistent performance over all angles in the horizontal plane; however, directional antennas should perform better in a dynamic propagation environment. A linear array antenna, one type of directional antennas, can perform

dynamical change horizontal pattern by simple changes of parameters of input signals. The later section includes (1) identifying antenna parameters based on locations of a vehicular transmitter and fixed receivers and (2) an approach to find parameters that needs for a linear array antenna. Through the simulations with our approach and realistic scenarios, the desired array pattern can be achieved and required parameters can be calculated. Based on the simulation results, DSRC is preferred to use in the scenario which contains large number of users, and LTE is preferred to use with wider bandwidth and smaller cell size. Also, the approach to find the controllable array antenna can be developed to the actual implementation of hardware.

Acknowledgements

I thank God for great people who helped me along my Master study and will help for future PhD study, too. I thank to my advisor, Dr. Carl Dietrich, who advised me for many researches and provided good opportunities in many research areas. I was able to learn many through the opportunities that he gave to me. Through the chances, I could strength my skills. I also thank to Dr. Jeff Reed and Dr. Vuk Marojevic for serving on my committee, and also thank to Dr. Harpreet Dhillon for serving on the chair for my Qualifying exam.

I thank to my parents, Yong-seok Choi and Eunkyung Choi, for all supports and opportunities for me to study in U.S. It is hard to send me to a foreign country and continuously support for studies.

I thank to my coworkers, Dr. Xiaofu Ma, Mo Kim, Chris Rowe, Biniyam Zewede, and Aakanksha Sharma. It was great time to discuss new research topics and work together for such long project.

Finally I thank to Federal Railroad Association who supported my research assistantship for many years.

Table of Contents

List of Figures

List of Tables

Chapter 1. Introduction/Motivation

1.1 Technological Views for Studying 5G

Commercial cellular wireless communication system evolved from first generation (1G) analog telecommunications to the current 4th generation (4G), long-term evolution (LTE), and is still in a process of continuous evolution. Fifth-generation (5G) wireless systems are expected to extend and improve upon current 4G LTE cellular systems; among these improvements, 5G wireless systems expected to improve latency to 5ms from 25ms, increase peak data rate to 10 Gbps from 100 Mbps [1]. As shown in Figure 1, 5G will be an improvement over 4G in many ways including features such as increased throughput, decreased latency, enhanced support for machine-to-machine (M2M) communications, and coexistence and interoperability among heterogeneous networks [1], [2]. The expected 5G will completely outperform the current 4G service, especially on the supporting number of devices, the volume of mobile data, and the peak data rate [1]. Due to the magnitude of the improvement from the current quality of service for 4G to the expected quality of service for 5G, a significant amount of investigations is needed for moving toward 5G. In 5G, the system mainly aims for a high integration with other wireless devices: any new 5G air interfaces, sharing a spectrum of LTE and WiFi, flexible and intelligent sharing [2]. As 5G gets more flexible in the future, shown in Figure 2, it will develop the capability to support a very wide range of services: Gigabit per second data throughput, smart city camera, self-driving car, augmented reality, etc. [3]. To develop the supporting infrastructure, extensive research is required to reduce

latency, increase reliability, handle more devices in the same network/cell/spectrum and to develop a new design for the coexistence of other wireless standards [3].

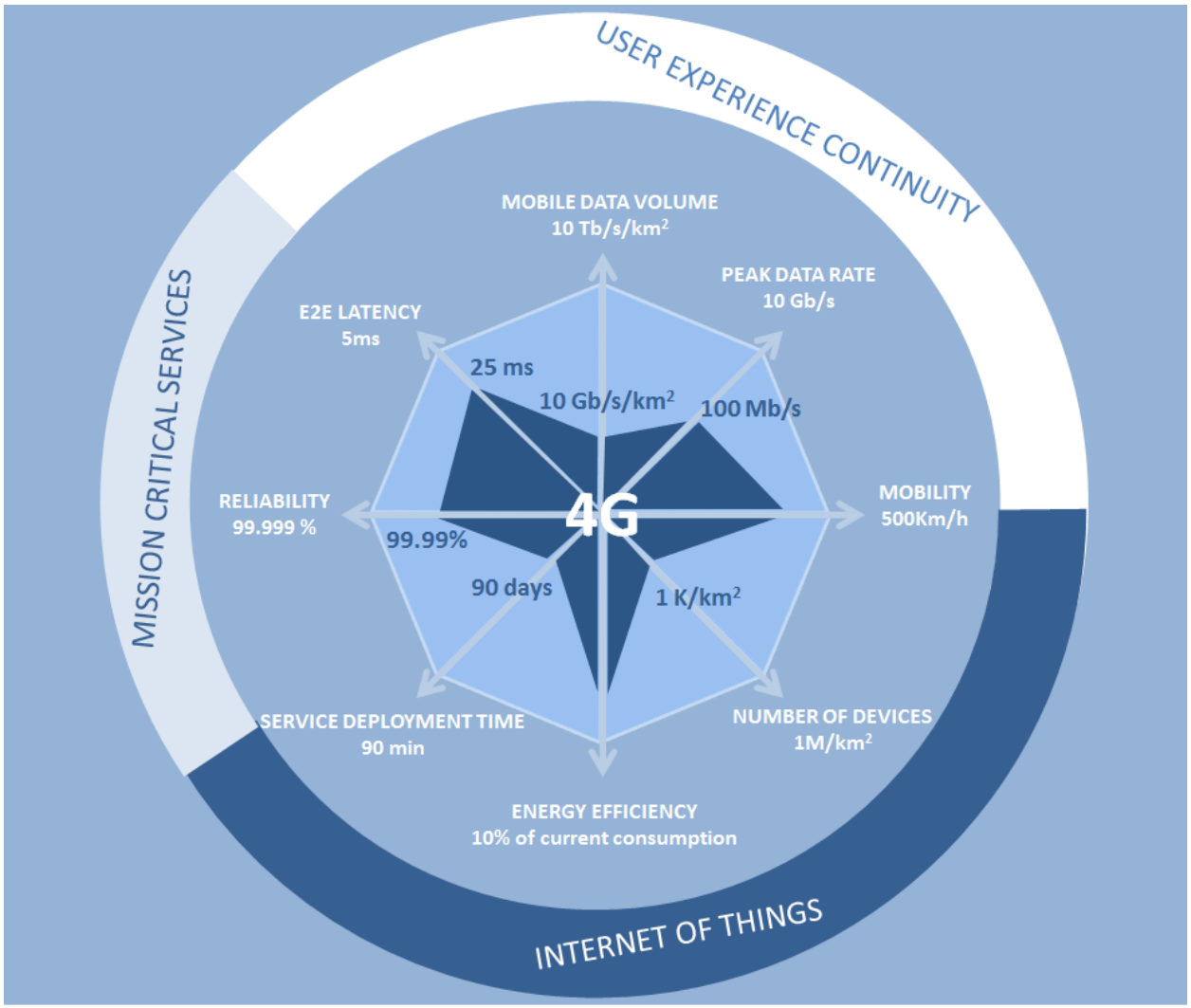

Figure 1 Diagram of 5G disruptive capabilities [1]

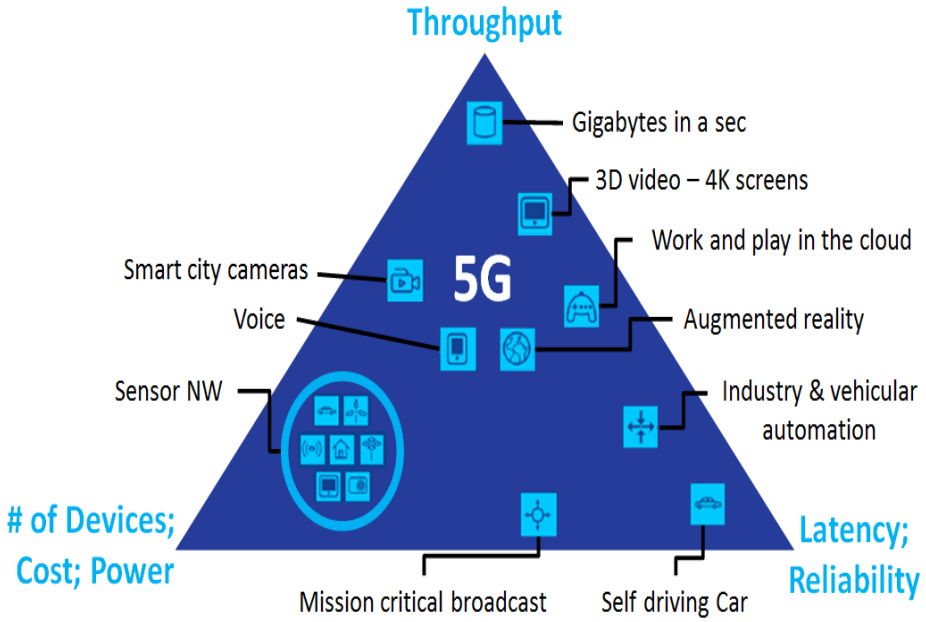

Figure 2 Diversity of services [3]

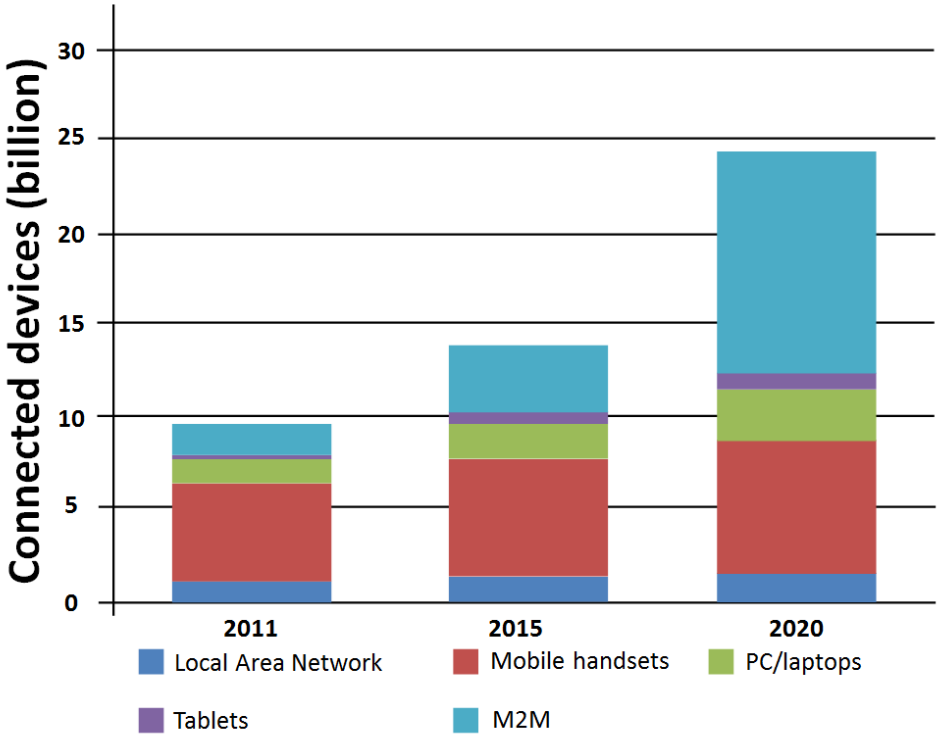

Figure 3 Expected number of devices [4]

The number of mobile handsets for 2011 was about 6 billion and the number is expected to increase to about 8 billion at 2020 [4]. However, as shown in Figure 3, the number of devices that require M2M connectivity is 2 billion in 2011 and expected to increase to about 15 billion at 2020 which is directly relevant to why the research for M2M should be more focused [4]. One application for 5G systems is the Internet of Vehicles (IoV), which refers networking technologies that support effective communication between vehicles [5], an extension of Intelligent Transportation Systems (ITS) that will connect vehicles to one another, to transportation infrastructure, and to a wide range of non-vehicular wireless devices. Dedicated Short Range Communications (DSRC) is a current standard for ITS applications, so it is a natural candidate for use in IoV systems. DSRC is using center frequency of 5.9 GHz and family of WiFi. It has been deployed to the market and slowly growing its usages. DSRC is using OFDM and has similar standard aspects with already existing WiFi standard. Also, its structure is somewhat simpler than currently deployed wireless communication systems such as LTE. However, cooperation with other systems will be required to augment DSRC's limited range, and to enable communication with a wide range of non-vehicular users and devices. While approaches for connecting vehicles to the IoV via 5G wireless systems are yet to be standardized and then commercialized, LTE and DSRC cooperative systems would suggest the possibility of IoV via 5G wireless systems.

The distinctive end-users of IoV will be vehicles and drivers, but IoV also has a potential to enable communications between road vehicles and pedestrians, trains, ships, airplanes, unmanned aerial vehicles, and much more. This is referred to as Vehicle-to-Everything (V2X). V2X enables numerous convenient, but not necessarily time-critical applications

and services. V2X system designs must consider and prove effective for critical safety warning applications.

1.2 Safety Issues

As shown in Table 1, in the United States, pedestrian deaths comprised 14% of total traffic fatalities in 2011, an increase of 3% from 2002, and 4,743 U.S. pedestrians were killed in traffic accidents in 2012 [6], [7]. As shown in Table 1, The total number of traffic fatalities decreased from 43,005 to 32,367 in 2002 to 2011, a decrease of nearly 25%, while a more modest 8.6% decline occurred in pedestrian fatalities during the same period, from 4,851 to 4,432 [7]. These reports emphasize an urgent need and an opportunity to develop Vehicle-to-Pedestrian (V2P) communication, one example of V2X, to improve pedestrian safety. Nearly 80% of United States railroad grade crossings are classified as 'unprotected' with no signals, warnings, or gates. Between January and September 2012, about 10% of the all reported railroad accidents and nearly 95% of all reported fatalities were a result of train-to-vehicle collisions [8]. These reports show the importance of Vehicle-to-Railroad (V2R) communications, which is another example of V2X. These reports prove V2X application should consider not only the system aspects, but also consider warning system for the safety of vehicle-related users.

The considerable metrics for LTE-DSRC cooperation models for warning systems are latency, network size, cost, market deployment, user capacity, and performance. The proper comparison between new considering model and existing models are needed.

In this thesis, we contribute to latency suggestions for the system and dynamic beamforming antenna to improve a performance of the system. In chapter 2, the related works about cooperative system models, latency suggestions, and dynamic beamforming

will be discussed. In chapter 3, the considerable factors when modelling the cooperative model which will be latency, communication reaching size, packet structure, and cost. In chapter 4, the details about simulators for DSRC and LTE will be present. The setups, results, and contributions through simulations also present. In chapter 5, the process about how to find desired angles of beam pattern by locations of nodes will be shown. The mathematical approach to find the weights of elements to get desired beam patter also is shown.

Table 1 Total Fatalities and Pedestrian Fatalities in Traffic Crashes 2002~2011 [7]

Year	Total Fatalities	Pedestrian Fatalities	Percent of Total Fatalities
2002	43,005	4,851	11
2003	42,884	4,774	11
2004	42,836	4,675	11
2005	43,510	4,892	11
2006	42,708	4,795	11
2007	41,259	4,699	11
2008	37,423	4,414	12
2009	33,883	4,109	12
2010	32,999	4,302	13
2011	32,367	4,432	14

Chapter 2. Background and Related Work

2.1 Studies about suitability of LTE or DSRC or cooperation for vehicular communication

There are many discussions about which technology is more suitable for ITS. Currently, the standard used for ITS systems is IEEE 802.11p, DSRC, which mainly used for V2V and V2I communication. Most of the studies compare IEEE 802.11p and LTE as two candidates for future ITS standard; however, these studies do not have all common decision. While a few conclude that IEEE 802.11p only is most useful for ITS, e.g., [9], some conclude that LTE is suitable for ITS and should be used alone [10], [11], [12]. However, other studies concluded that a combination of LTE and IEEE 802.11p will generate better performance for ITS [13], [14], [15].

Few studies agree that using DSRC itself for vehicular communication is better. In [9], the author compared the performance of a vehicular ad hoc network (VANET), based on IEEE 802.11p, and infrastructure-based centralized LTE by sending continuous beacons. The author of [9] concluded that an LTE network is easily more overloaded, bad communication, than VANET under ideal assumptions. However, the authors of [10], [11], [12] contradict this assertion, concluding that LTE is more suitable for ITS. In [12], the author compares performance of LTE and IEEE 802.11p using a ns-3 simulator with three different performance metrics: end-to-end delay, packet delivery ratio, and throughput. The author concludes that IEEE 802.11p is more sensitive to larger vehicle densities, traffic load, and vehicle speed than LTE. Therefore, the author of [12] conclude that LTE is more suitable for ITS; however, the author further conclude that for smaller

vehicle densities, IEEE 802.11p can offer good performance to support ITS. In [11], the author proposed mechanisms for broadcast LTE-direct transmissions with two phases: Resource allocation and Distributed Resource Access Scheduling. Gallo *et al.* concludes that by the flexibility of the network resource allocation mechanism and independent distributed access scheduling, extended studies of LTE can be more suitable for vehicular safety communications. In [10], the author evaluates the technical feasibility of the combination of cloud-based servers and LTE cellular networks for vehicular safety communication. By evaluating using performance metrics such as maximum number of UEs supported, traffic, and round trip latency, it shows that LTE with MBMS/non-MBMS solutions can substitute vehicular safety communication.

Other studies [13], [14], [15] agree that LTE has better performance and is somewhat able to substitute for IEEE 802.11p in vehicular safety communication; however, at the same time, they argue that IEEE 802.11p can provide better performance than LTE for certain scenarios, so a combination of LTE and IEEE 802.11p is preferred for ITS.

The author of [13] analyzes the performance and behavior of LTE in ITS scenario by using LTE_ITS simulator and concludes that LTE can meet most requirements of ITS applications and it is possible to serve more users than IEEE 802.11p. Also, LTE can solve problems that IEEE 802.11p faces: contention delay, beacon collision, beacon loss, interference among users, etc. However, the author of [13] also concludes that IEEE 802.11p can offer much lower beacon latencies than LTE while LTE can provide larger capacity, communication range, and guarantee a minimum Quality of Service (QoS). The final conclusion is a combination of IEEE 802.11p and LTE standards for ITS; using IEEE 802.11p for serving the first class of ITS applications, the Cooperative road safety

applications and using LTE for the other two applications, Cooperative traffic efficiency class and Cooperative local services and Internet class.

In [14], Araniti *et al.* surveys LTE for the capability to support cooperative ITS and vehicular applications. The author expected that LTE plays a critical role in vehicular communications; however, it only applies to rural areas where population and UE density is low. The author expected cooperative communication with IEEE 802.11p to give better performance, for example, LTE can be helpful at intersections and in non-line-of-sight conditions and provides wider coverage. In [14], Araniti *et al.* concludes that more discussion is needed regarding cooperative systems that employ IEEE 802.11p and LTE for ITS, addressing architectural design, vehicular device deployment, and that resource management and more effective business models should be specified to ensure that someone will agree to pay for the services.

In [15], LTE is evaluated for ITS based on performance in field-measurements. The measurements were performed while driving at 60mph and measured inside and outside of the vehicle. The author provided a small-cell deployable ITS model with backhaul and compared DSRC and LTE. Moreover, the author of [15] concluded that IEEE 802.11p is suitable as a technology for time-sensitive automotive applications that require low latency and high reliability and LTE is suitable for non-time-sensitive applications. As these authors discussed, there is no definite answer for the future ITS standard. However, a combined system of LTE and IEEE 802.11p is needed because LTE and IEEE 802.11p can offset each other's disadvantages.

There are many studies for pedestrian safety from vehicles; however, only a few considered DSRC and LTE cooperative systems. LTE and DSRC cooperation system is

modeled in [16]. Several studies about V2P applications, such as [17], [18], and [19], do not rely on coexisting LTE and DSRC systems. However, in [19], the author claims a partial LTE and DSRC system, whereas it addresses the potential after combining the two popular standards which are more valuable in discussing the guideline of a future V2P network systems.

In [16], Atat *et al*. provides a cooperative model of LTE and IEEE 802.11p for vehicular communication in which LTE is used for long range communication and IEEE 802.11p is used for cooperation on short range communication. In [16], the author concluded that the best performance occurs when the base station unicasts to a selected vehicle for long range and the selected vehicle multicasts to other vehicles for cooperation. The concept of a cooperative model is particularly interesting because of the detailed descriptions of LTE and DSRC roles and how these systems can cooperate. In [17], the author showed the possibility of using Wi-Fi equipped devices for vehicular safety communication. Also, in [18], Tornell *et al.* showed that use of smartphones to provide ITS warning service can result in much safer systems. In [19], the author showed a detailed approach for a V2P system using IEEE 802.11g, GPS, Wi-Fi, and an Android smartphone. It also provided a model for a Wi-Fi based pedestrian protection application. While [17], [18], [19] are relevant to V2P warning systems, they do not employ coexisting LTE and DSRC systems. Honda has developed technology for V2P systems and a system for V2P and Vehicle-to-Motorcycle (V2M) communication [20]. The system uses DSRC equipped vehicles and smartphones, which requires installing Honda's application [20]. The system uses GPS signals to determine locations of pedestrians and warns both drivers and pedestrians [20]. Although reference [20] is an example of LTE and DSRC system cooperation. While

installation of a custom smart phone application is straightforward, the system's major limitation is that it initially supports only Honda products.

2.2 Studies about Architectures / Models for IoV

One interesting IoV application is discussed in [18], which presents detailed device requirements for V2P and an algorithm based on geographical destination area (GDA). The system is based on Wi-Fi and GPS, which is conceptually similar to our cooperative LTE-DSRC system. Reference [18] also shows the requirement of warning time based on the location of vehicle and pedestrian. Another study proposes V2R communications using LTE [21]. The authors developed a LTE Railway (LTE-R) testbed which allows analyzing different cell deployment procedures and optimization. They found that LTE can be adapted for railway safety applications. Ucar *et al.* [22] present hybrid architecture for VANET safety which is based on DSRC and LTE. Their architecture involves the cooperation of DSRC and LTE as cluster networks. Their focus is on system reliability and performance evaluation with many different parameters such as cluster head duration, delay, data packet delivery ratio; whereas our focus is on two critical metrics for warning system performance, service reliability, and latency. These references and the increasing pervasiveness of LTE confirm that LTE and DSRC are two standards that can enable V2X communications and underline the need for establishing key performance metrics and thresholds to ensure that V2X systems are designed to support safety warning applications.

We consider future communication system for V2X that comprises cooperating LTE and DSRC systems. Many studies of cooperative LTE and DSRC systems have targeted different topics including better performance and new cooperation models [12], [16], [23],

[24], [25], [26]. Interestingly, the general ideas of cooperated models represented in these references are somewhat similar to each other. As shown in Figure 4 and Figure 5, cooperation models from the references can be categorized into two major models: a vehicle-cluster model and an individual vehicle model.

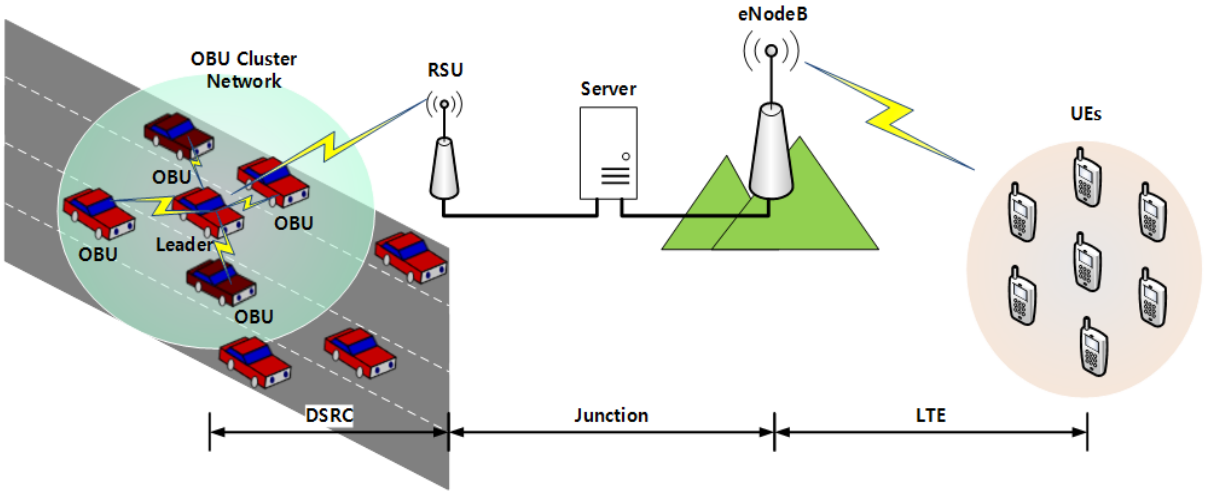

Figure 4 LTE and DSRC Cooperation Model Category 1 (Cluster Model)

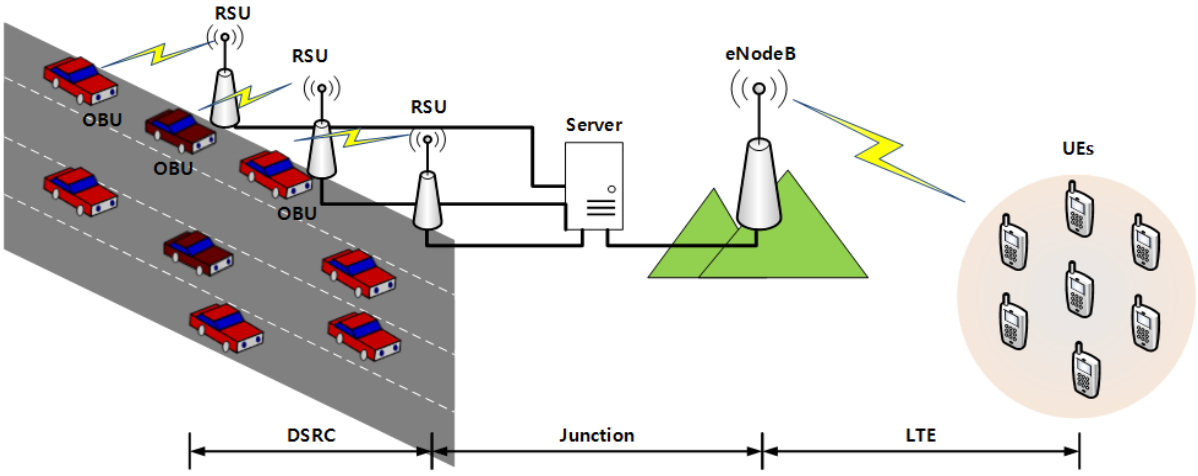

Figure 5 LTE and DSRC Cooperation Model Category 2 (Individual Model)

The elements of both models are vehicular On-Board Units (OBUs), one or more Road-Side Units (RSUs), a server that acts as a bridge between DSRC and LTE, an LTE

eNodeB, and LTE user equipment (UEs). The LTE side has one eNodeB (base station) and several UEs (e.g., handsets) which exist in one cell, as usual in an LTE communication system. The DSRC network in Figure 4 comprises one RSU and multiple OBUs and is a clustered network, in which one vehicle has the role of cluster leader, and only the leader communicates with the RSU and broadcasts to other nearby OBUs. The DSRC network in Figure 5, which depicts the individual vehicle model, includes multiple RSUs and multiple OBUs. The RSUs are equally spaced to provide continuous communications along the road. The junction subsystem has the role of connection between the DSRC and LTE networks. In Figure 4 and Figure 5, the junction is represented as a 'server'; however, it can also be a cloud network, the Internet, or physical TCP/IP connection to an ITS center server. The models from other studies differ in the method used to connect DSRC and LTE at the junction. Thus, the choice of the best method for the junction subsystem is the most effective way to optimize overall system performance.

2.3 Studies about Antennas for Vehicular Communication

Currently, vehicular communication systems are using omnidirectional antennas for consistent performance regardless of vehicle orientation. However, moving vehicles tend to face complex geographical locations for communication with other radios. The complex locations may have different fading environment which will decrease efficiency of communication. A directional antenna with a dynamically synthesized pattern can target the receiver, increase throughput and gain, and reduce delay.

Most of the smart antenna studies for LTE and IoV communication systems are proposed on the receiver side [27], [28]. The authors of [27] show simulation studies on array

receiver antenna by using Direction-of-Arrival (DOA) algorithms. The proposed antenna is for 3G network and beyond. The authors are interested in generating multi-dimensional array antenna by the DOA algorithm and its performance by Bit-Error-Rate (BER) for certain noise while we are interested in finding out the array elements' weight. The authors of [28] proposed group-based channel access scheme with using a smart antenna on the infrastructure side. In the design of the system, infrastructure uses a smart antenna, which is a directional antenna with controlling power gain, and vehicles use an omnidirectional antenna. Their proposed system is similar to ours by the scenario, V2I; however, they implemented smart antenna on the infrastructure side, receiver, while we are interested in the transmitter side, on vehicle. Reference [29] is much similar to our contributions. It proposed adaptive array antenna by using Invasive Weed Optimization (IWO) algorithm to set maximal gain and null at a certain point. The algorithm is interested in where to put null and max gain; no interconnection with the location of receiver or transmitter. Reference [19] shows a system that is Wi-Fi based Vehicle-to-Pedestrian Communications. Their system is interested by each node use GPS device and by the location information, their algorithm can be calculated a threshold for a warning. But it does not considered antenna aspect; it is more focused on warning system based on location. Even they did not consider antenna part for communication; the idea of synchronizing GPS device and radio nodes is interested.

Chapter 3. Considerable Factors when Modelling LTE and DSRC Cooperation System

Standards that are major candidates to provide vehicular communications for ITS will be evaluated using several performance metrics. Comparison of performance metrics is required to make decisions regarding which system will be more efficient and / or more effective, and which system should be adopted. Possible performance metrics are latency, traffic efficiency, network size, cost, capacity, market deployment, mobility support, QoS support, broadcast type, V2I/V2V support, etc. [14]. Using these performance metrics, the ITS systems can be compared fairly. The two main candidate standards of ITS, IEEE 802.11p and LTE, are compared based on performance metrics, as shown in Table 2.

The systems are fairly comparable with the performance metrics; however, the priority of metrics is different. For example, the highest priority performance metric for a vehicular communication system when used for transferring files or music will be throughput and latency; however, the highest priority performance metric for the system for sharing traffic information will be the probability of success, which includes upper limits on latency as well as packet error rate (PER) for a given distance and associated warning time. Defining the priority of performance metric for a given system or application is important.

Table 2. Configuration Comparison of IEEE 802.11p and LTE

Metrics	IEEE 802.11p	LTE
Bandwidth	10MHz	1.4, 3, 5, 10, 15, 20 MHz
Frequency Range	5.86-5.92 GHz	7000-2690 MHz
Bit Rate	3-27Mbps	Up to 300 Mbps
Coverage Range	Up to 1km	Up to 30km
Broadcast/multicast Support	Native broadcast	Through eMBMS
V2I Support	Yes	Yes
V2V Support	Native (ad hoc)	No
Market Penetration	Low	High

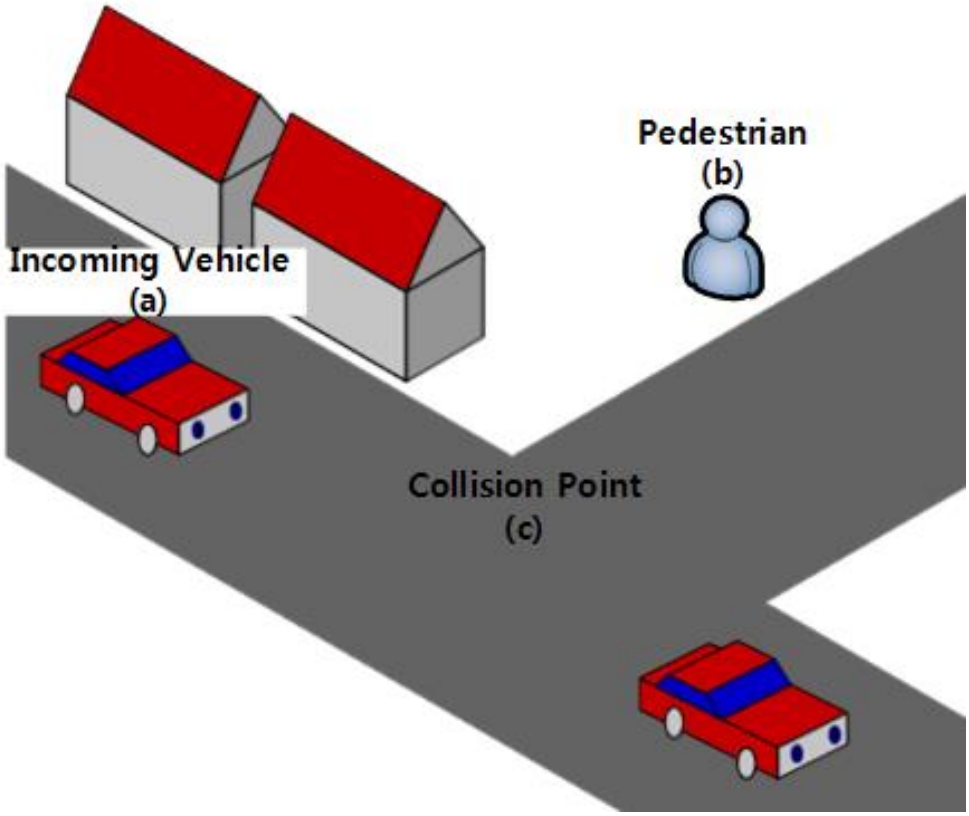

Figure 6 V2P Pedestrian Warning Simplistic Scenario

3.1 Latency

Latency is one parameter related to QoS. It is the time required to complete a whole communication message transfer, transmission to reception (end-to-end latency). The latency may be a minor factor to consider; however, it becomes a major considerable factor when the application is a warning system. Because of the difference appearing by usage in LTE-DSRC cooperation system applications, the survey of a proper requirement of latency for each application is needed. Short latency of system is surely good for any application, but there will be unnecessary extra effort may appear to decrease latency and some trade-off may occur. The major source of latency is more likely from Medium Access Control (MAC) layer delay compared to PHY layer, which is appearing same for both LTE and DSRC; the packet of LTE and DSRC should contain certain necessary messages, and the length of packet affects latency.

As Figure 6 shows, the main elements for a V2P pedestrian alert system are the projected or potential collision point (c), referred to simply as the collision point, the incoming vehicle, and the nearby pedestrian. The system's purpose is to warn the pedestrian and / or driver to recognize whether a pedestrian is nearby or a vehicle is incoming so that both pedestrian and driver can carefully / safely pass the collision point. For the V2P alert system, safety requirements dictate a maximum acceptable delay. If the delay value of the system does not meet the requirement, either a driver or a pedestrian may act too late to avoid an accident. Therefore, the system timing requirement, delay, needs to be discussed. The scenario of interest for the V2P alert system is defined as follows: A vehicle and a pedestrian are moving in such a way that they will meet at some point, the collision point (c), and some time, $Time_{vehicle\ collide\ to\ pedestrian}$, if their trajectories do not change. Further,

both driver and pedestrian should recognize each other's presence by the alert. $Time_{vehicle\ collide\ to\ pedestrian}$ should be examined to find the upper limit of latency of the system. Let the distance between incoming vehicle, point *a*, to collision point, point *c*, be d_{ac} and the distance between pedestrian, point *b*, and collision point be d_{bc}. The time that vehicle collides to pedestrian is:

$$Time_{vehicle\ collide\ to\ pedestrian} = \frac{d_{ac}}{velocity_{vehicle}} + \frac{d_{bc}}{velocity_{pedestrian}} \qquad (1)$$

For both driver and pedestrian safety, all system processing should consume much less time than $Time_{vehicle\ collide\ to\ pedestrian}$. Since the system involves reactions from people, a human factor delay will occur. That delay may be as long as a few seconds and is a major component of the overall delay. The human factor delay is expected to be highly variable depending on parameters such as user reaction time, a state of user alertness and / or distraction, and the device application and its user interface. Therefore, we concentrate the current study on the communication system latency, $Time_{Total\ Communication\ Delay}$, with the goal of minimizing this latency to allow as much time as possible for variability in the human factor delay within the overall requirement that the combined warning and reaction time must be much less than $Time_{vehicle\ collide\ to\ pedestrian,}$ because of the possibility of randomness and uncertainty of human factor delay, which will be more than communication system delay:

$$Time_{vehicle\ collide\ to\ pedestrian} \gg Time_{Total\ Communication\ Delay} \qquad (2)$$

The larger difference between $Time_{vehicle\ collide\ to\ pedestrian}$ and $Time_{Total\ Communication\ Delay}$ will provide better service and a safer system by enabling both pedestrians and drivers to have more time to react. The $Time_{Total\ Communication\ Delay}$ can be considered as end-to-end delay that occurs in communication between the radio in the vehicle and the radio that the pedestrian carries. Similar to other vehicle-related applications, more time between the total collide time and the communication delay, it will provide more time for the safety.

3.2 Communication Range

Communication reaching size is the range of displacement of transmitter and receivers. Depends on the size of the network, the system architecture, propagation model, and population of nodes will change. In this DSRC system case, different size of a network will affect the number of population in the network and propagation model. In this LTE system case, different size of a network will affect system architecture, such as microcell or macrocell scenario, a number of UEs in the network, and also propagation model. The network size should be defined mainly by the number of targeted users in the network, and then other factors, system architecture, and propagation model, need to follow by the size category.

Broadcasting warning messages through VANET, also an example of V2X, needs to send messages to broader than V2P, which is more focus on one cross section. Also, the size to cover for V2R or V2V will be different due to the vehicle and railroad's different speed and different time to approach the danger point. Therefore, sufficient network size should be known and apply differently for other applications.

3.3 Packet Structure

DSRC and LTE have different messages contained in their packet. DSRC contains information which is more relevant to vehicular information such as GPS longitude, latitude, vehicle heading, and acceleration. LTE has more freedom to contain message than DSRC's packet. The proper selection of message into a payload of each packet is required when studying for LTE and DSRC cooperative system. Fortunately, both LTE and DSRC are using OFDM, which is the effort to create new packet is less than two standards that are using the different type of communication system.

Also, the customized packet should consider the performance of communication system in both LTE and DSRC side. DSRC packet size is usually 100~300 bytes long which is shorter than LTE packet size. The smaller packet size can reduce latency more than longer packet; however, it can contain less information. The studying of a proper relationship between packet size, latency, and QoS is needed.

3.4 Cost

Since LTE and DSRC are the separated systems, the cooperated system requires radios that can work both LTE and DSRC; the cost of the system will be more than one standard communication system. Moreover, the cost will be directly proportional to implemented nodes of radio. For example, the system is one way broadcasting system, the only cost elements will be broadcasting tower and user devices. For another example, the system is targeting for vehicles, road infrastructure, and pedestrians, the cost elements will be radios that will implement inside of a vehicle, infrastructure which will act as a relay, and user devices that pedestrians will carry. The user of the application will impact the needed elements of the system and it will affect the total cost of the system.

One other factor relevant to the cost of the system is market deployment ratio. Reuse of the devices that were already deployed to users and use them as part of LTE-DSRC cooperative system for V2X will reduce many costs instead of deploy all radio nodes for a new system. Therefore, when designing a new model, the standard system which is already deployed in the market well will be a good candidate to be a base standard for the system.

Chapter 4. Survey of LTE and DSRC Latency

The previous section includes latency sources for cooperative LTE and DSRC models. The equations mentioned in the previous section are for large networks as shown in Figure 4 and Figure 5. This section will discuss suggestions of reducing the delay in DSRC and LTE.

4.1 DSRC Simulations

This section is about the descriptions of DSRC standards, the simulator descriptions, the setups for simulations, and the results.

4.1.1 DSRC PHY Simulator

This section is about the descriptions of DSRC standards and simulator/simulations for PHY layer.

A. DSRC PHY Standard

The IEEE 802.11p standard is an amendment to IEEE 802.11-2007 for Wireless Access in Vehicular Environments (WAVE) applications [30]. It combines a variation of the IEEE 802.11a PHY layer with the IEEE 802.11e MAC layer [31]. The signal processing of IEEE 802.11p is the same as the processing of IEEE 802.11a, OFDM PHY as shown in Figure 7. However, IEEE 802.11p allocates 10 MHz bandwidth for each individual channel while IEEE 802.11a uses wider channels of 20 MHz bandwidth. Also, the subcarrier spacing and the data rate of IEEE 802.11p are half of IEEE 802.11a's specification, but symbol interval including cyclic prefix (CP) is doubled [30]. More specific compared values between IEEE 802.11a and IEEE 802.11p are shown in Table 3.

As shown in (Table 3), the parameters for IEEE 802.11a and IEEE 802.11p are almost identical except for doubling in time units and halving for frequency units. These changes have been made in order to mitigate the effect of frequency-selective fading and thus accommodate the high mobility of vehicular networks.

For PHY layer simulation, only one transmitter and one receiver are necessary. The transmitter and receiver design for IEEE 802.11p includes the same functional blocks as the design of IEEE 802.11a, and both of them use OFDM in the PHY layer. OFDM PHY Tx contains encoder, interleaver, mapping, IFFT, and OFDM modulator. OFDM PHY Rx contains decoder, deinterleaver, demapping, FFT, and OFDM demodulator. Figure 7 shows transmitter and receiver block diagrams for OFDM PHY.

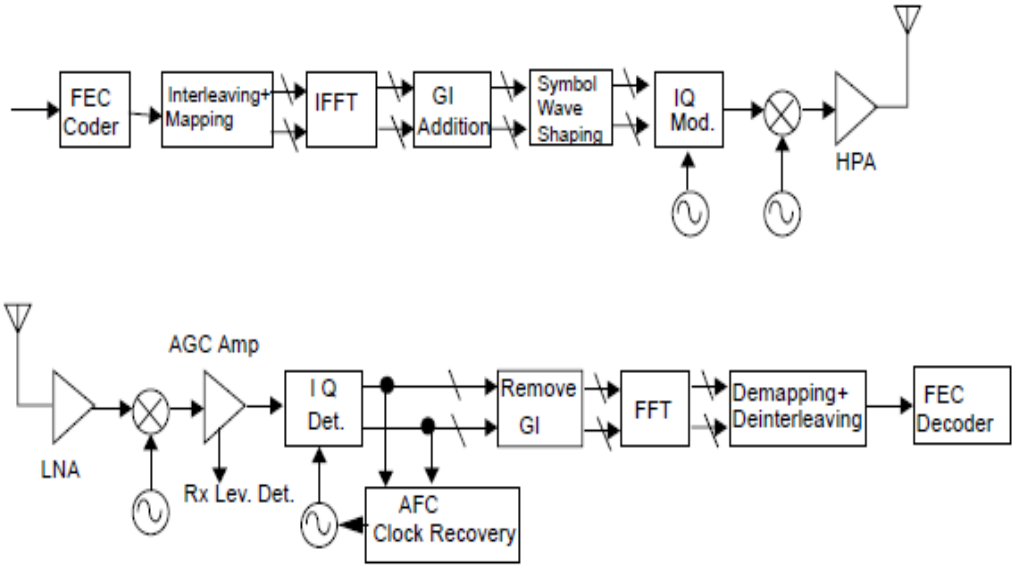

Figure 7 Transmitter and Receiver Block Diagram for OFDM PHY [27]

The OFDM PHY's Forward Error Correction (FEC) coder uses a convolutional code with K=7 and available coding rates are R=1/2, 2/3, or 3/4. Also, the convolutional encoder uses the generator polynomials g_0=133 and g_1=171. In Figure 8, output data "A" shall be

output from the encoder before the output data “B”. A Viterbi decoder is recommended to use since convolutional encoder is used.

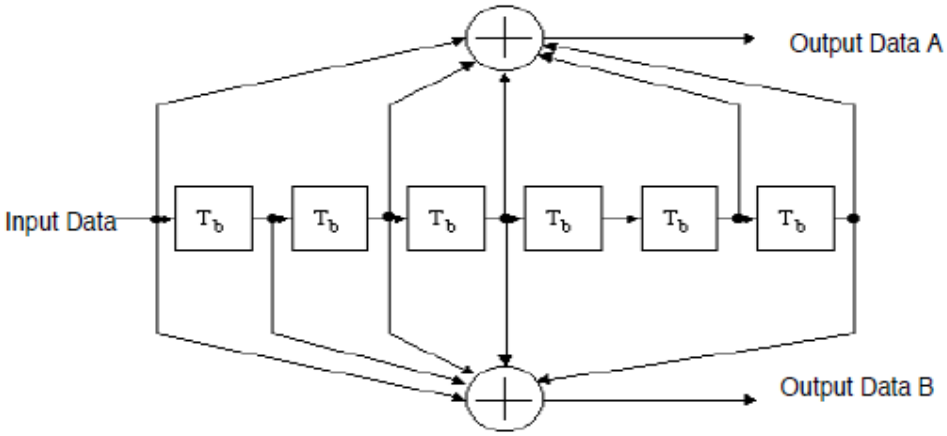

Figure 8 Convolutional Encoder (k=7) [32]

All encoded bits are interleaved to a block size corresponding to the number of bits in one OFDM symbol. Bits in one OFDM symbol differ based on the combination of modulation schemes and coding rate.

48 data subcarriers, 4 pilot subcarriers (which are located on subcarriers -21, -7, 7, and 21), one null subcarrier, and 11 subcarriers for the guard are in one OFDM symbol that has 6.4μs period time. After creating one OFDM symbol, a guard interval and preamble are inserted.

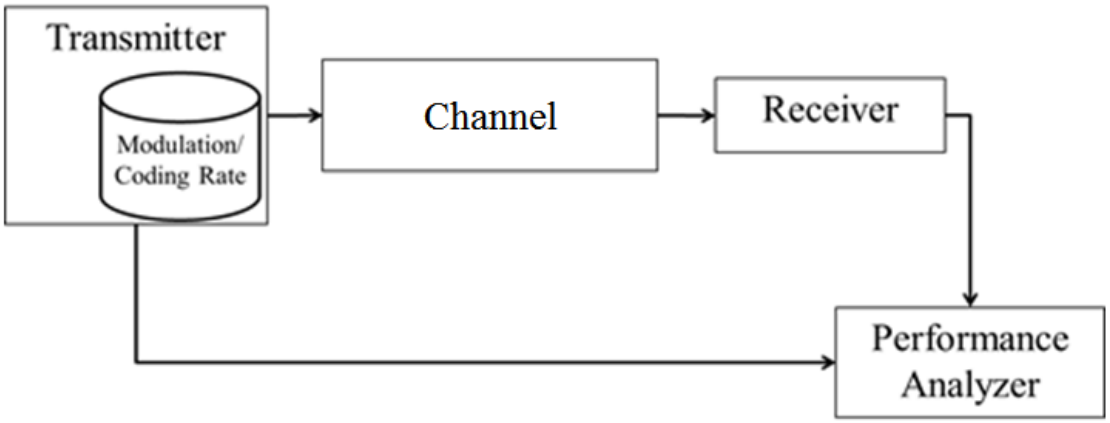

Figure 9 Block Diagram of DSRC PHY Simulator

B. DSRC PHY Simulator Description

The IEEE 802.11p simulator is modified from an IEEE 802.11a simulator which is provided by Matlab Simulink [33]. The simulator is fully implemented in software, Simulink, and it contains one transmitter, one receiver, modulation/coding rate controller, noise environment selection, and performance analyzer. Figure 9 shows a block diagram of the whole simulator.

Table 3 Comparison between IEEE 802.11a and IEEE 802.11p

	IEEE 802.11a	**IEEE 802.11p**
Bandwidth	20 MHz	10 MHz
Bit Rate	6, 9, 12, 18, 24, 36, 48, 54	3, 4.5, 6, 9, 12, 18, 24, 27
Modulation Scheme	BPSK, QPSK, 16 QAM, 64 QAM	BPSK, QPSK, 16 QAM, 64 QAM
Code Rate	1/2, 2/3, ¾	1/2, 2/3, 3/4
# of Subcarriers	52	52
# of Data Subcarriers	48	48
# of Pilot Subcarriers	4	4
Subcarrier Spacing	0.3125 MHz	0.15625 MHz
FFT Period	3.2 μs	6.4 μs
FFT/IFFT Size	64	64
Guard Time	0.8 μs	1.6 μs
Preamble Duration	16 μs	32 μs
Symbol Duration	4 μs	8 μs
Signal Field Duration	4 μs	8 μs
CP Interval	0.8 μs	1.6 μs
OFDM Symbol Interval	4 μs	8 μs
Max EIRP	800 mW	2W

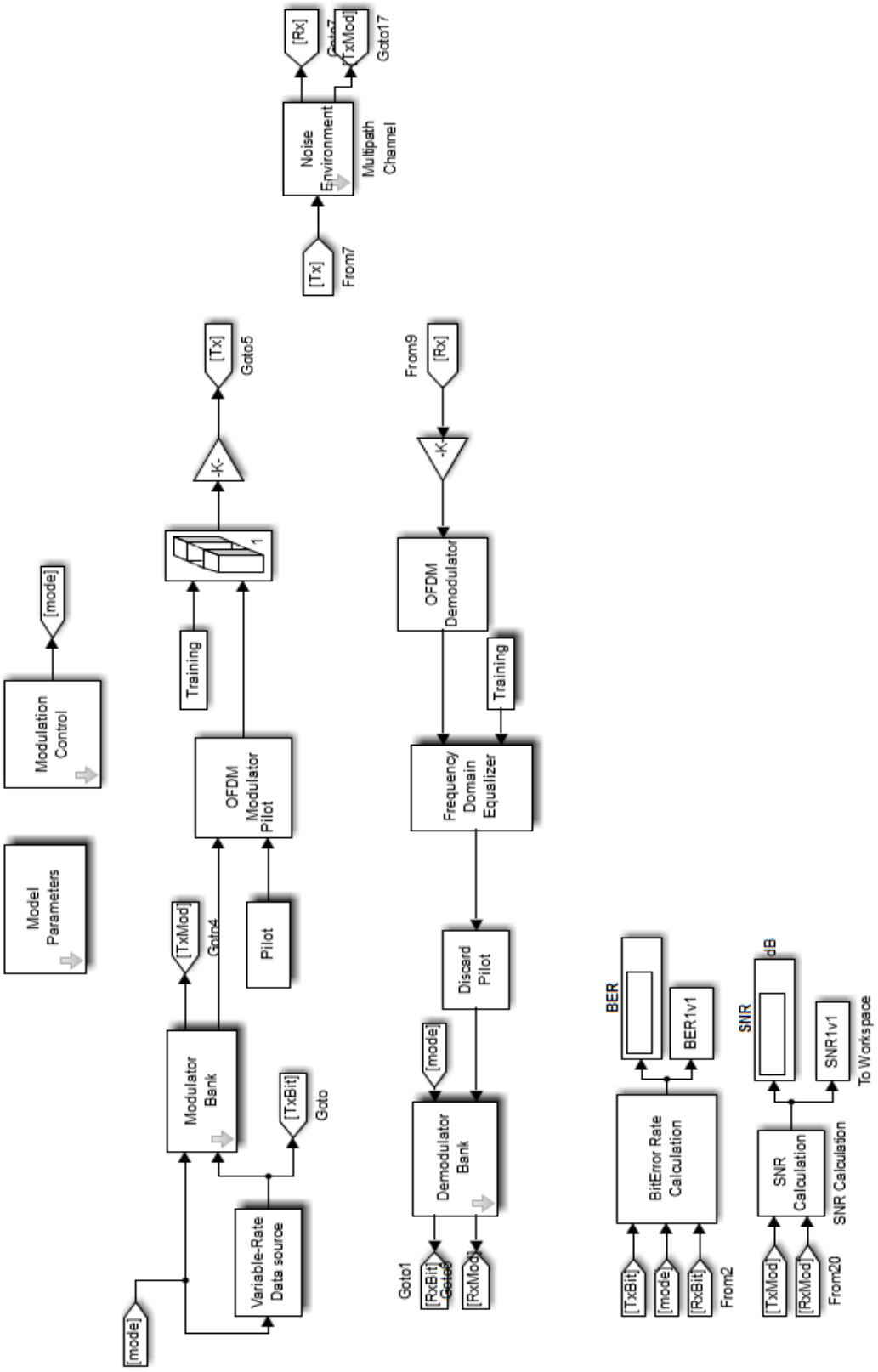

Figure 10 Simulink DSRC PHY Simulator

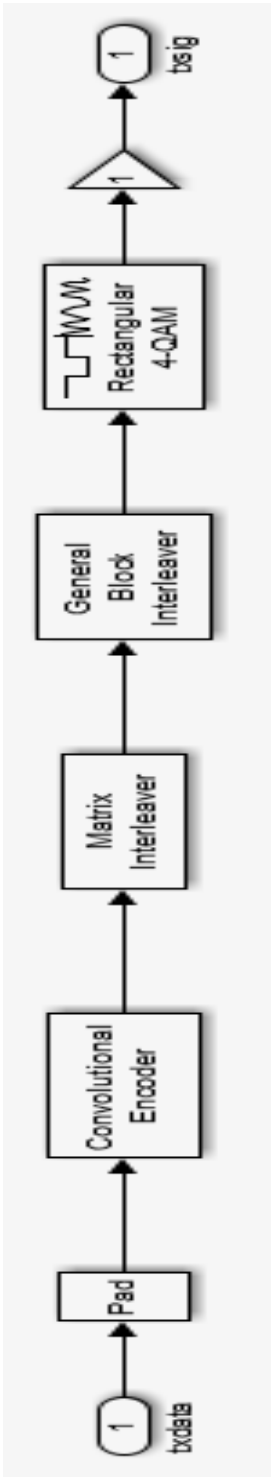

(a)

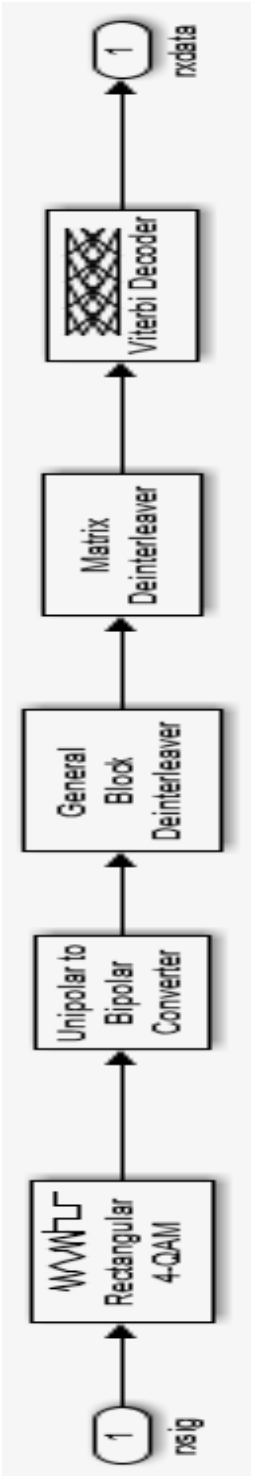

(b)

Figure 11 DSRC PHY (a) Tx (b) Rx Design

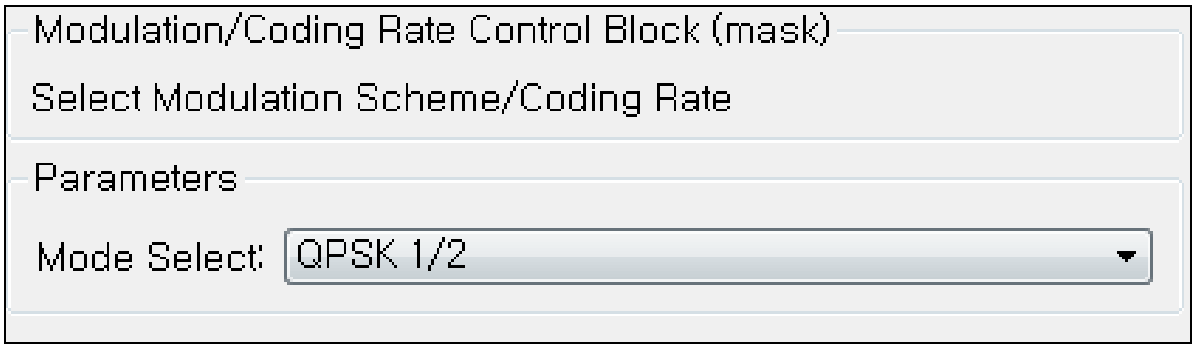

Figure 12 Modulation/Coding Rate Control Block

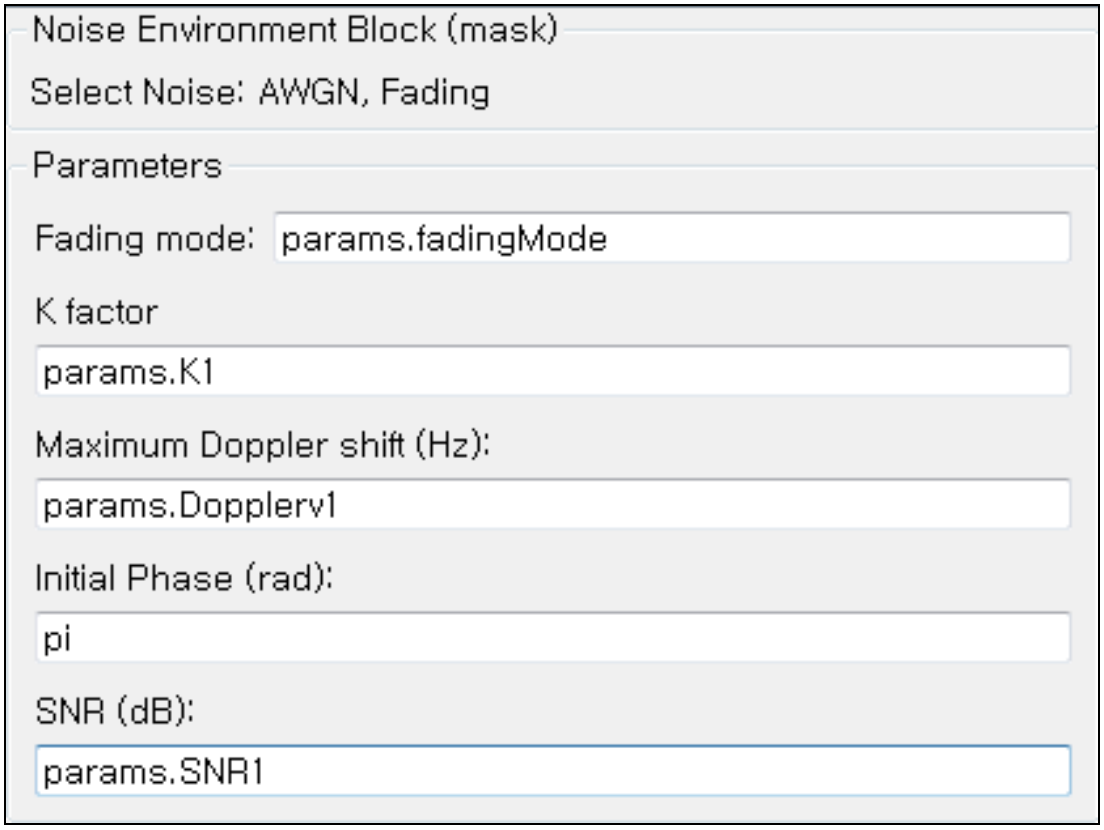

Figure 13 Noise Environment Block

```
% IEEE 802.11p - fundamental sizes
p.NFFT         = 64; % Number of points on FFT
p.CPLen        = 16; % Cyclic prefix length
p.guardBands   = [6; 5]; % Left and right guard bands
p.pilotIndices = [-21; -7; 7; 21]; % Pilot subcarrier indices

% OFDM symbols
p.OFDMSymPerFrame    = OFDMSymPerFrame;
p.OFDMTrainPerFrame  = OFDMTrainPerFrame;
p.OFDMTotSymPerFrame = OFDMSymPerFrame + OFDMTrainPerFrame;

% Modulator/demodulator banks
p.numModulators = 8;
p.txBitsPerSymbol = [1 1 2 2 4 4 6 6];
p.txBitsPerBlock = p.numTxSymbols * p.txBitsPerSymbol;
p.modOrder = 2.^p.txBitsPerSymbol;
p.codeRate = [1/2 3/4 1/2 3/4 1/2 3/4 2/3 3/4];

% Timing-related parameters
p.OFDMSymbolPeriod = 8e-6;

% Noise-related parameters
p.fadingMode=1; % 1 for No fading 2 for Rician fading
p.K1 = 1; % K-factor parameter for Fading option
p.K2 = 2;
p.Dopplerv1 = 5.463*16;
p.Dopplerv2 = 5.463*40;
p.SNR1 = 26;
p.SNR2 = 25;
```

Figure 14 Initialization m file

Figure 10 is a Simulink model of IEEE 802.11p PHY, which I developed and based on an existing 802.11a PHY model [33] as described previously. The simulator contains Tx, Rx, modulation control block, Figure 12, noise environment block, Figure 13, BER calculation, and SNR Calculation blocks. Middle upper long series of blocks are Tx of IEEE 802.11p PHY and lower long series of blocks are Rx of IEEE 802.11p PHY. The modulator block, Figure 11 (a), contains convolutional encoder, interleaver, and modulation selections which are defined by modulation control block, Figure 12. Similar to modulator block, demodulator block, Figure 11 (b), contains Viterbi decoder, deinterleaver, and demodulation selections which are also defined by modulation control block. Modulation/Coding Rate control block, Figure 12, has selections to choose one from BPSK 1/2, BPSK 3/4, QPSK 1/2, QPSK 3/4, 16-QAM 1/2, 16-QAM 3/4, 64-QAM 2/3, and 64-QAM 3/4. Noise environment block, Figure 13, is able to select AWGN only or fading with AWGN. Once fading is selected, k factor, maximum Doppler shift, initial phase, and SNR can be numerically defined by a user. Initialization m file, Figure 14, can edit a number of points on FFT, cyclic prefix length, guard bands, OFDM symbols, symbol timing, etc. The simulator runs by steps: setting parameters in initialization m file, modulation control block, noise environment block, then running.

C. Transmitter Block

The Transmitter block performs the following tasks: random bit generation, pilot addition, training sequence addition, OFDM, and modulation. It can also adapt to preselected modulation schemes and coding rates. The available options are BPSK 1/2, BPSK 3/4, QPSK 1/2, QPSK 3/4, 16-QAM 1/2, 16-QAM 3/4, 64-QAM 2/3, and 64-QAM 3/4. The modulation scheme also decides the number of bits per OFDM symbol: 1, 1, 2, 2, 4, 4, 6,

and 6 respectively. Each OFDM symbol has 48 data subcarriers, and each frame has 20 OFDM symbols. Therefore, total bits per each frame are 480, 720, 960, 1440, 1920, 2880, 3840, and 4320 respectively. The randomly generated digital signals will be modulated through modulation, OFDM modulation, pilot addition, and training sequence addition process and transmitted.

D. Noise Environment Block

The Noise Environment Block performs the function of selecting a user-defined noise (and/or fading) environment. Since DSRC is mainly designed for vehicular communication, fading is generally the dominant propagation phenomenon. DSRC is usually Line-of-Sight (LOS) communication, so Rician fading is more common than Rayleigh fading. Therefore, the simulation is mostly focused on Rician fading with various parameter values. As already mentioned, the block possesses both fading functionality and Additive White Gaussian Noise (AWGN) functionality. The reason for existence of AWGN is not only to create realistic noise environment but to also compare the performance between IEEE 802.11p and IEEE 802.11a in the absence of fading. By the noise environment block, the simulator can run in different realistic noise environments which can be controlled by users.

E. Receiver Blcok

The Receiver performs OFDM demodulation, training sequence removal, discarding of pilot and demodulation functionalities. The receiver also has a copy of the original bits that were subjected to noise and fading, to be used as a reference by the performance analyzer.

The performance analyzer has two major inputs: the randomly generated bits at the transmitter and the bits after the receiver. Also, it possesses the information as to which modulation scheme and code rate have been used, and uses this for calculations. The main purpose of the performance analyzer is to measure Signal-to-Noise-Ratio (SNR), calculate E_b/N_0 and find the Bit-Error-Rate (BER). Using data collected from performance analyzer, the simulator can then visualize the performance. The performance of DSRC PHY layer simulators over AWGN, Rician and Rayleigh fading channel with different parameters, and effect of modulations and coding rates can be shown in Appendix B.

4.1.2 DSRC MAC Simulator

The DSRC MAC layer simulator is based on a Carrier Sensing Multiple Access with Collision Detection (CSMA/CD) method. The main input of the simulator is Packet Error Rate (PER) for a channel model of interest, a number of nodes, and the location of each node. The simulator provides the latency of each node as a result. The simulator is done in Matlab script. The algorithm of the simulator is several nodes of DSRC start transmission, sense medium, check delay counter, transmit message, and continue the loop; much detail is shown in Figure 16, and the protocol Matlab script is shown in Appendix C. The relationship between DSRC PHY simulator and DSRC MAC simulator is shown in Figure 15. By providing PER values from PHY layer, receiver nodes will perform based on the given values.

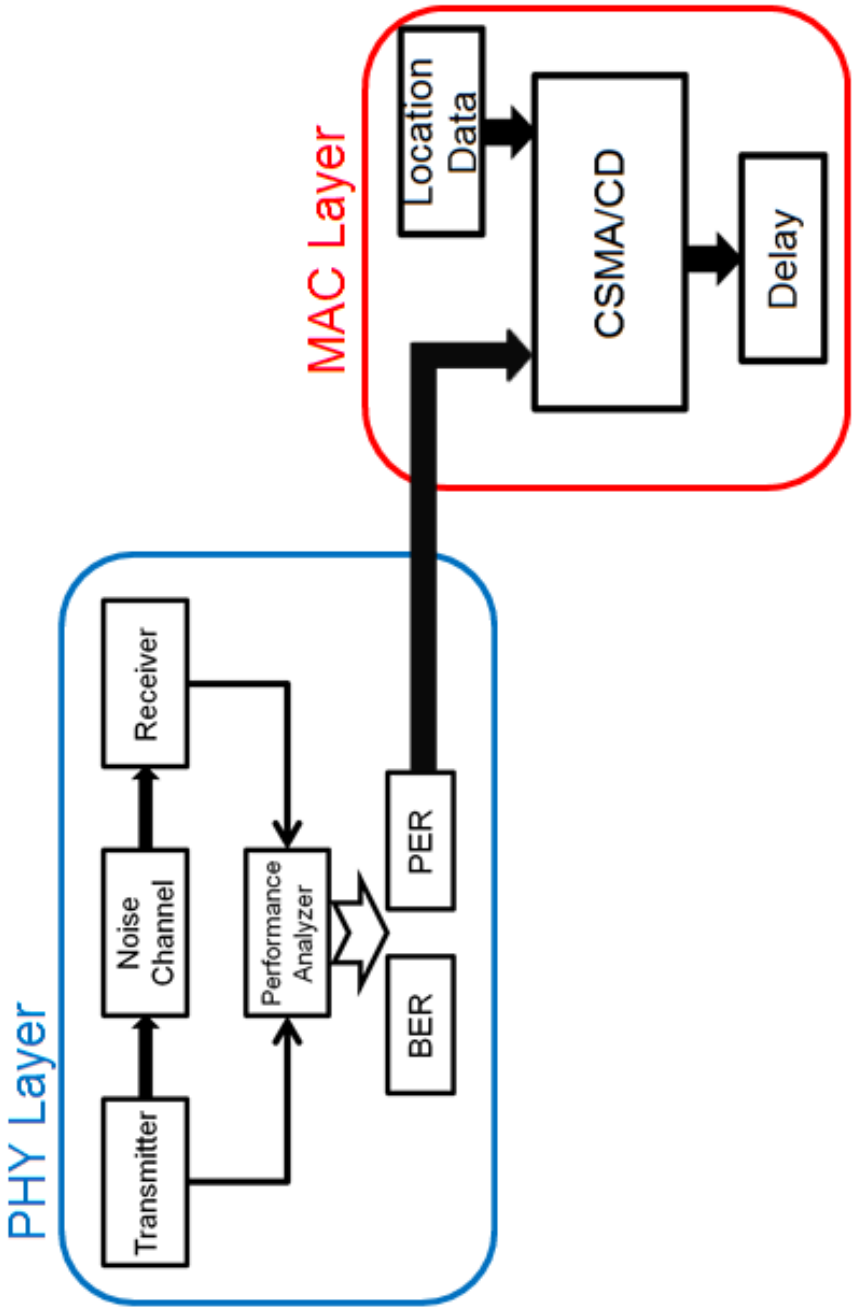

Figure 15 DSRC PHY and MAC Relationship

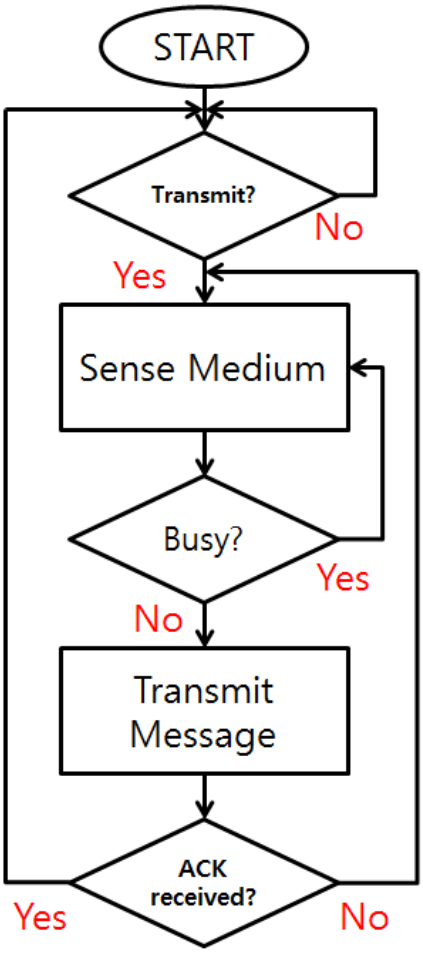

Figure 16 DSRC MAC Layer simulator algorithm

4.1.3 DSRC Simulation Settings

DSRC simulations were performed to find out suggestions to reduce latency for LTE-DSRC cooperative system. The usual communication range of DSRC is approximately 300m. The simulation used a DSRC MAC layer simulator. PER for a particular channel model is collected from DSRC PHY layer simulator [34], and the adapted channel model is HIPERLAN/2 model C, 5GHz large open space environment for NLOS conditions and 150ns average rms delay spread [35]. More detail values for HIPERLAN/2 model C is

shown in Appendix A. Figure 17 shows the compared PHY later simulation result and result from [36]; the result is collected by running simulator with the setup of modulation of 16-QAM, a coding rate of 1/2, and 54bytes/packet.

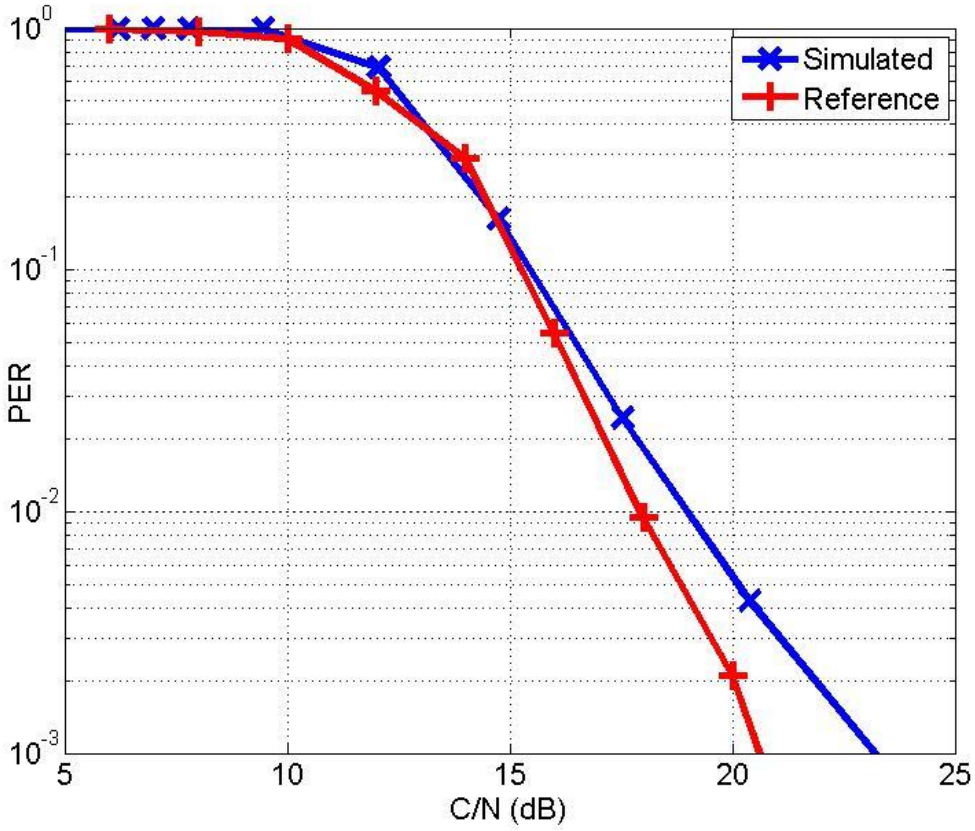

Figure 17 DSRC PHY Layer Simulation result for HIPERLAN/2 model C

In the simulator, the parameter *priority* controls the transmission time ratio compared to simulation time; higher *priority* tends to provide more frequent opportunity to transmit. The MAC layer simulator ran with an EIRP of 33dBm, which is the typical power level for private communication using DSRC. Half of the nodes were placed within 100 m from the transmitter and the other half of the nodes were placed in a range between 100 and 300 m. Without loss of generality, these ranges were chosen since they are

representative for low speeds, e.g. a pedestrian or car approaching a railroad crossing. Two cases are compared here: In case (1), nodes both inside and outside of the 100 m range have the highest *priority*, and in case (2), the nodes inside the 100 m range have the higher *priority* than the nodes outside the 100 m range. For both cases, the transmitter is placed at the center of the simulation field and all other receiver nodes are randomly placed in either inside of 100m range or outside of 100m range; the number of nodes that are placed in/out are the same. Figure 18 and Figure 19 are showing the placement of transmitter node and receiver nodes with priority.

Table 4 describes more detailed parameters for the DSRC as well as the LTE simulation setups. Figure 20 and Figure 21 show average delay vs. the number of DSRC nodes.

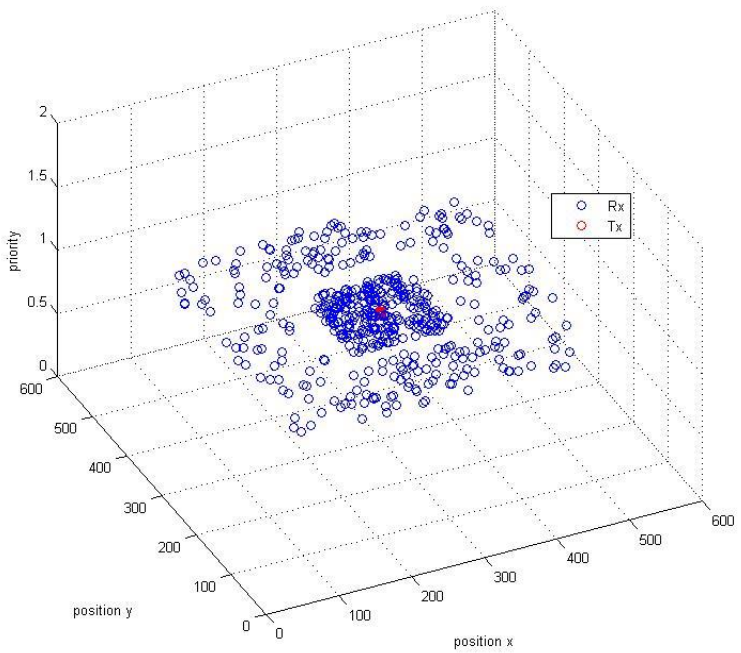

Figure 18 High/High Priority

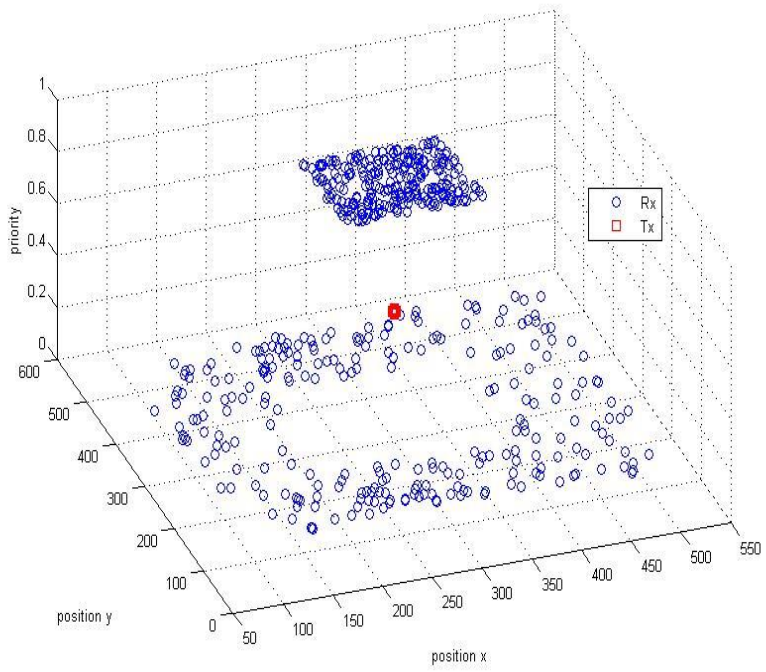

Figure 19 High/Low Priority

Table 4. MAC Layer Simulation Parameters

	Inside 100m	Outside 100m
Packet Size	200 bytes/packet	200 bytes/packet
Channel Model	HIPERLAN/2 model C	HIPERLAN/2 model C
EIRP	33dBm	33dBm
# of nodes	3,4,5,10,15,20,25,30,35,40,45,50, 55,60,65,70,75,86,100,113,125	3,4,5,10,15,20,25,30,35,40,45,50, 55,60,65,70,75,86,100,113,125
Priority	High	High/Low
Loss Source	Path Loss, Fading	Path Loss, Fading

4.1.4 DSRC Simulation Results

Both Figure 20 and Figure 21 show average delay for all nodes, nodes inside 100m, and nodes outside 100m.

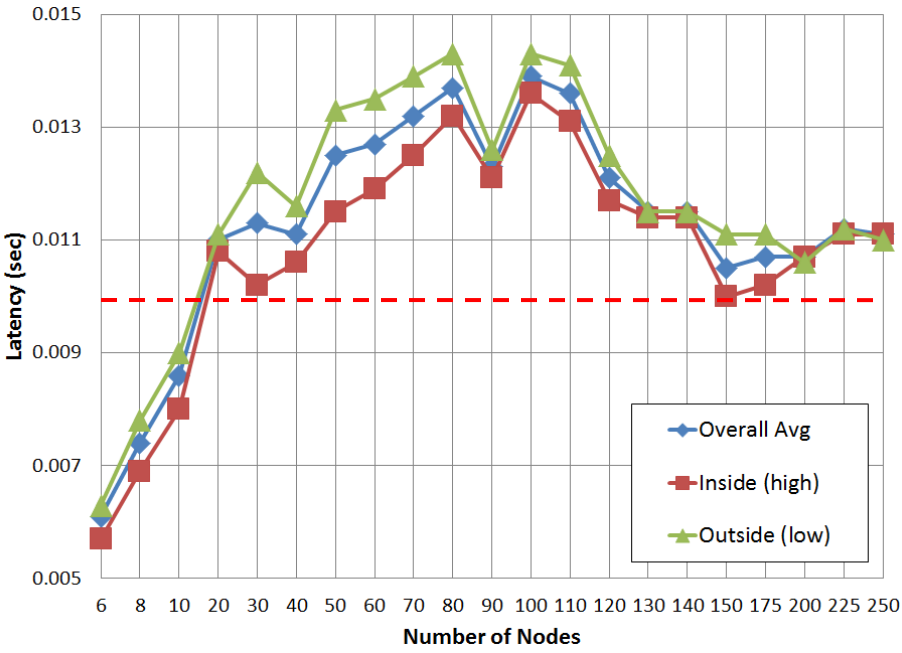

Figure 20 Average & Range of delay for High priority inside 100m and Low priority outside 100m (red line indicates 10ms, DSRC standard latency limit)

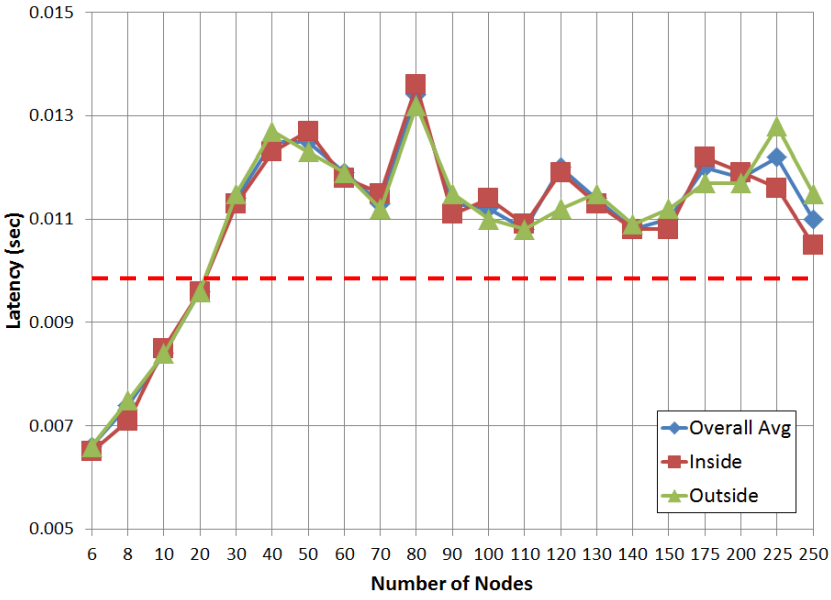

Figure 21 Average & Range of delay for High priority inside and outside 100m (red line indicates 10ms, DSRC standard latency limit)

As shown in Figure 20, higher *priority* users have lower latency than lower *priority* users. As shown in Figure 21, if the nodes have the same *priority*, the latencies for nodes inside and outside the 100m radius are about the same. Also, we can see that the distance between transmitter and receiver does not affect latency; nodes that are at different locations but have the same *priority* experience a similar latency (Figure 21 (b)). Interestingly, DSRC latency increases with the number of nodes, but established around 0.011 seconds (+/-10%) for around 30 or more nodes. We expected that the latency would keep increasing the number of users in the network.

From these simulation results, we notice that the *priority* has a larger effect on the latency than does distance between the radios. Also the latency is stable for a large number of users. Therefore, DSRC can be a good option for the warning scenario where a large number of users in a network exist with high *priority*.

4.2 LTE Simulations

This section is the descriptions of the LTE simulator, SimuLTE, the setups of simulations, and the results.

4.2.1 LTE Simulator

The simulation ran with SimuLTE [37], open source LTE simulator. The simulator, for a single cell downlink scenario, contains a server, a router, an eNodeB, and UE nodes. The user can control parameters such as the number of UEs, cell size, transmit power, channel model, carrier frequency, and gain of antennas. SimuLTE can generate network model and reuse the created model for a network. The LTE simulations are done with Single Cell Downlink scenario, the network is shown in Figure 22, and the network is composed

of a single LTE model, which is shown in Figure 23. The network contains server, router, eNodeB, and UE, and when the network is generating, server, router, and eNodeB are shared and a user defined number of UEs are generated for the network. The channel parameters, such as pathloss scenario, eNodeB/UE antenna gain, etc., network size, a number of UEs, and cell size are able to be set by user's preferences, see Appendix D. By the flexible parameter control, SimuLTE can run for desired network scenario. The results of the simulator are number of a sent packet, a number of received packet, queueing time for each node, throughput, end-to-end delay, packet loss, etc.

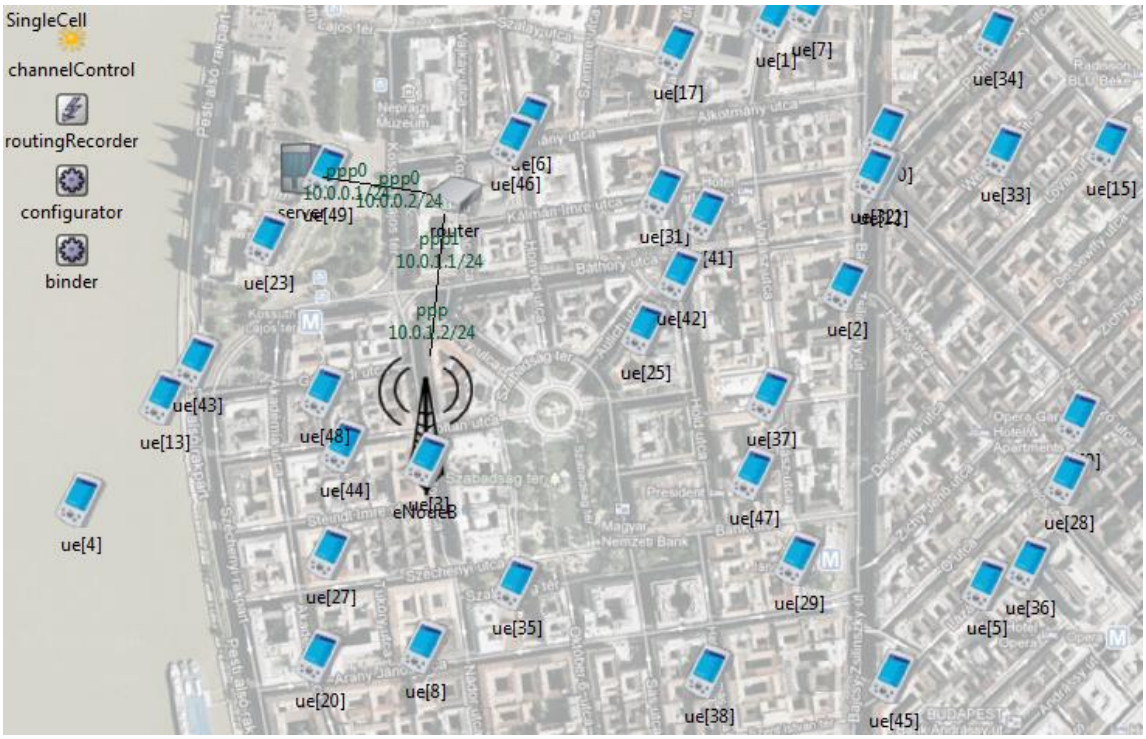

Figure 22 SimuLTE Single Cell Downlink network [37]

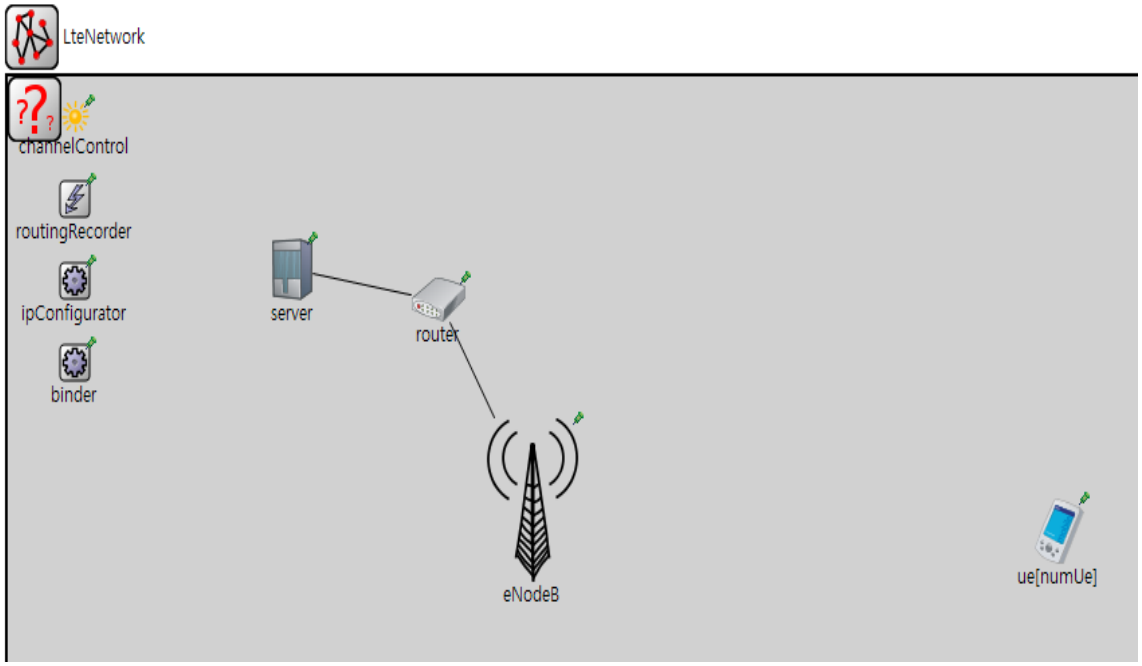

Figure 23 SimuLTE Single LTE Network Model [37]

4.2.2 LTE Simulation Setup

LTE simulations were performed to find the suggestions to reduce latency. An LTE packet size of 200 bytes, which is the same size as used in the DSRC setup, allows performance comparison. Unlike DSRC, LTE is more flexible in choosing parameters such as bandwidth, data rate, and cell size. We considered bandwidths of 5, 10, and 20 MHz, which are typical in commercial LTE deployments in the US and cell sizes of 300 m to observe the effect of bandwidth on latency. Also, we selected cell radii of 100, 300, 600 m, and 1 km for a 10 MHz LTE system to analyze the effect of cell size on latency. The more detailed parameters are shown in

Table 5.

Table 5. Parameters for LTE Simulations

Cell Radius	**100m**	**300m**	**600m**	**1km**
Transmit Power (W)	5W	5W	5W	5W
eNodeB gain (dBi)	18dBi	18dBi	18dBi	18dBi
Carrier Frequency	2.1GHz	2.1GHz	2.1GHz	2.1GHz
Bandwidth	5MHz, 10MHz, 20MHz	5MHz, 10MHz, 20MHz	5MHz, 10MHz, 20MHz	5MHz, 10MHz, 20MHz
Test Model	Urban Micro	Urban Micro	Urban Micro	Urban Macro
Fading Type	Jakes, LOS	Jakes, NLOS	Jakes, NLOS	Jakes, NLOS
Testing Scenario	VoIP	VoIP	VoIP	VoIP
Number of UEs	10, 20, 30, 40, 50, 60, 70, 80, 90, 100, 110, 120, 140, 150, 160, 180, 200, 230, 250	10, 20, 30, 40, 50, 60, 70, 80, 90, 100, 110, 120, 140, 150, 160, 180, 200, 230, 250	10, 20, 30, 40, 50, 60, 70, 80, 90, 100, 110, 120, 140, 150, 160, 180, 200, 230, 250	10, 20, 30, 40, 50, 60, 70, 80, 90, 100, 110, 120, 140, 150, 160, 180, 200, 230, 250

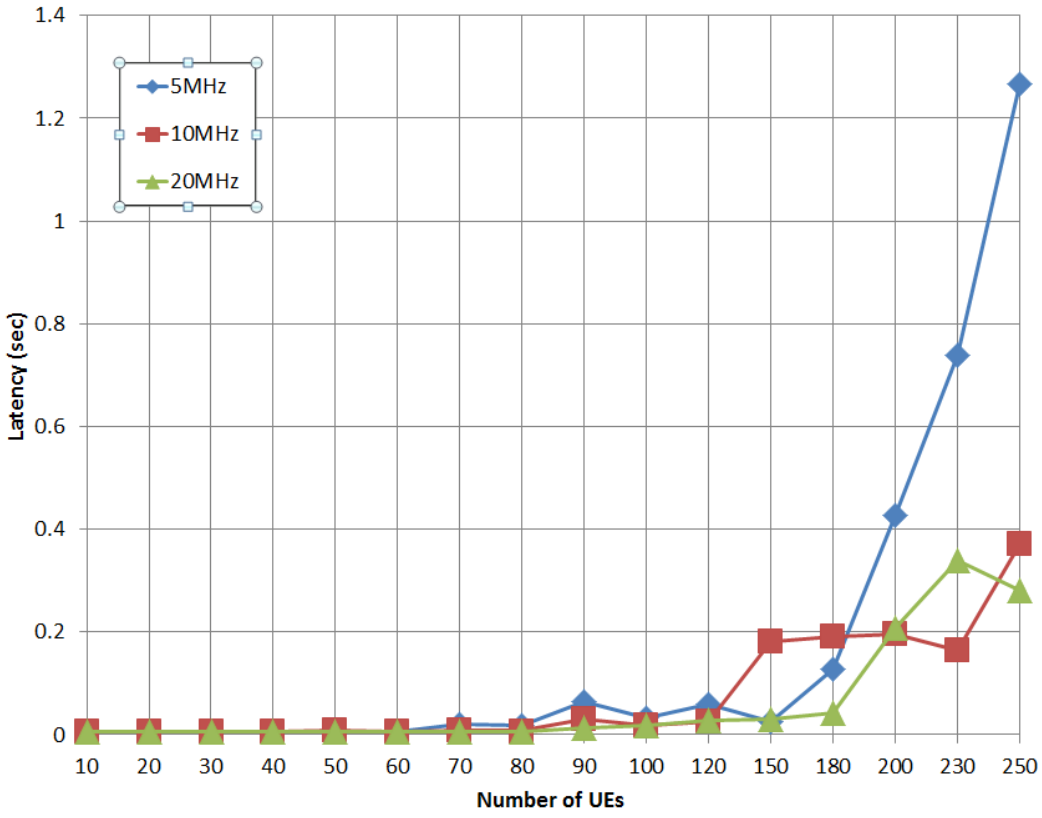

Figure 24 End-to-End delay for different numbers of UEs and signal bandwidths (230~240 is the limit capacity for VoIP)

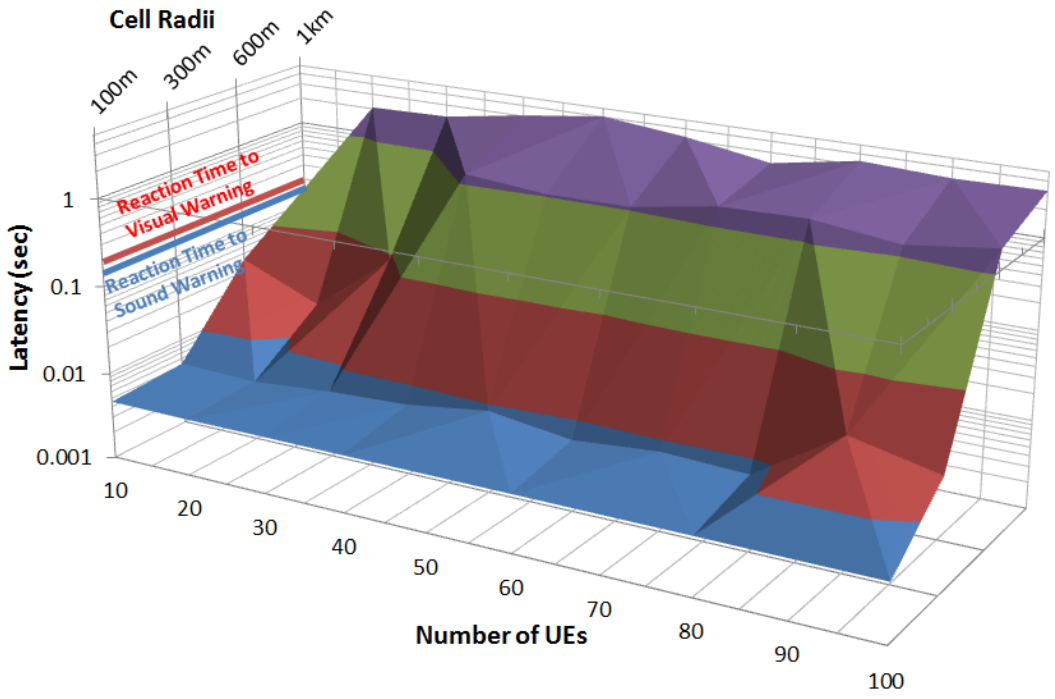

Figure 25 End-to-End delay for different number of UEs and cell radii

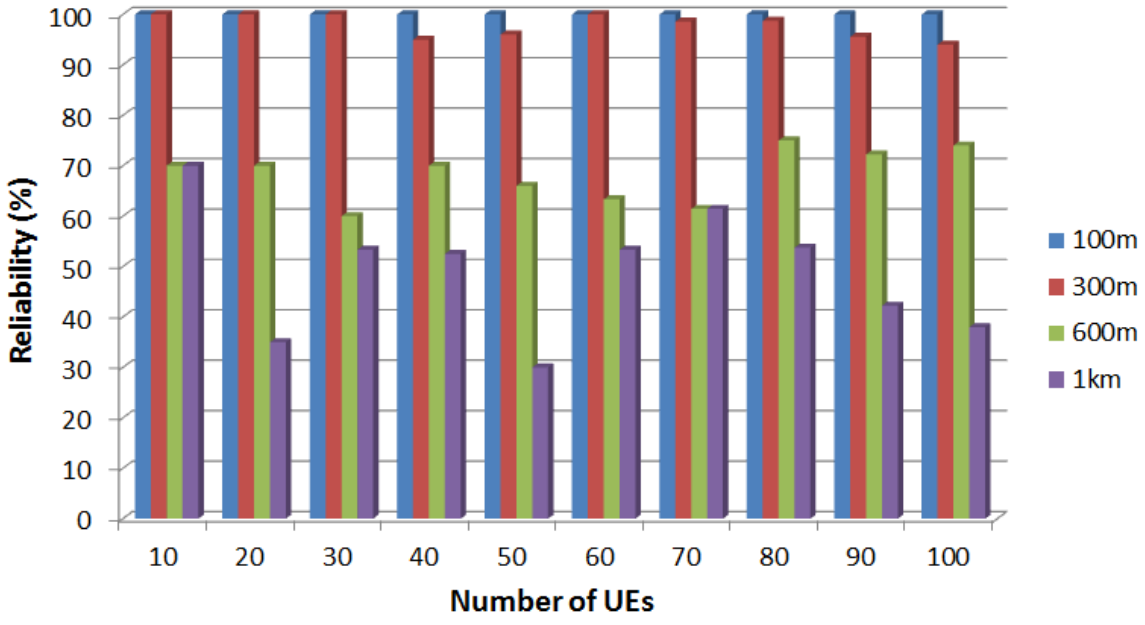

Figure 26 Reliability as a function of the number of UEs and cell radii

4.2.3 LTE Simulation Result

Figure 24 shows the end-to-end delay for successfully communicating users that use LTE signal bandwidths of 5, 10, and 20 MHz. For fewer than 120 UEs per cell, wider bandwidth results in lower latency. However, for a larger number of users the latency performance for 10 MHz and 20 MHz bandwidths are similar as opposed to the latency performance of 5 MHz LTE, which is worse. Figure 25 shows the end-to-end delay for successfully communicating users in cells that have radii of 100, 300, 600 m, and 1 km. Figure 26 indicates the system reliability in terms percentage of users who experience acceptable service. All of the LTE simulations used the same fading scenarios and physical parameters including the fading model, K factor, antenna gain, and transmit power. From these results, we conclude with several points:

- Wider bandwidth can provide better latency, as expected, as more resources are available to satisfy the user service requests. However, for a large number of users, increasing the LTE system bandwidth beyond 10 MHz does not significantly improve the latency figure.
- Figure 25 shows that the cell radius considerably affects the latency. Latency is similar for 100 and 300 m cell radius; however, the latency for a 1 km cell radius exceeds 1 s.
- Figure 26 indicates that the service quality is a function of the number of users, in general, but is much more pronounced for cell radii above 300 m.

From these results, we conclude that a wider system bandwidth reduces system latency if the active user population is below 100 users per cell. A narrow system bandwidth is detrimental for the system latency, particularly for a larger user population. However, cell

size impacts latency more than bandwidth. For numbers of UEs between 30 and 100, the latency shows little variation with the number of users per cell, but the average latency increases as the cell radius increases. Under the assumption of having the same channel environment and physical parameters, smaller cells can provide much better service to the users; the phenomenon shows that SNR does effect more to the performance than other factors.

Chapter 5. Dynamic Antenna for Vehicular Communication

Most commercial antennas are built with fixed size and fixed specifications. For example, a directional antenna such as a horn antenna is built with fixed power gain and pattern, as are omnidirectional antennas. Engineers must choose an antenna that is suitable for their purpose. Omnidirectional antennas cover all angles well, but their performance is lower than a directional antenna for many dynamic fading environments. However, directional antennas have low performance when the main beam is not oriented toward the target. A communication system such as the IoV involves transceivers that have high mobility, which leads to rapid variations in multipath fading, and requires the flexibility of an adaptive or smart antenna.

Linear array antennas are one type of antenna that can generate a variety of beam patterns by giving different weight to each element. We consider use of a flexible linear array antenna with controllable weights to satisfy desired antenna parameters based on GPS data.

To achieve system performance improvement by adapting the array antenna for the practical scenario, it is necessary to 1) predict the desired antenna pattern, which includes information about steering angle and beamwidth, based on real-time locations of devices; 2) calculate and apply the weights of the linear array antenna elements to synthesize a beam pattern with the desired parameters found from 1).

5.1 Mathematical Approach

In this section, we discuss (1) how to identify parameters of desired beamforming pattern based on GPS information and (2) how to derive the weight for each element of a linear

array antenna. The array antenna is a configuration of multiple radiating elements, and multiple small antennas are used in an array to achieve performance (characterized by parameters such as gain and beamwidth) similar to a single large antenna, but with greater flexibility. [38] As a starting point, we consider a linear array antenna, in which the center lays along a straight line [38]. The array factor of a linear array can be represented as:

$$AF = \mathrm{I}_o e^{j\xi_0} + \mathrm{I}_1 e^{j\xi_1} + \mathrm{I}_2 e^{j\xi_2} \cdots \tag{3}$$

$[\mathrm{I}_o, \mathrm{I}_1, \mathrm{I}_2 \cdots]$ represents a constant value of amplitude and phase shift. $[\xi_0, \xi_1, \xi_2 \cdots]$ represents phases of an incoming plane wave at each element.

We can rewrite array factor as a function of polar-coordinate angles as:

$$A(\phi, \theta) = a_1 e^{j2\pi d \sin\theta \cos\phi} + a_2 e^{j2 \cdot 2\pi d \sin\theta \cos\phi} + \cdots + a_N e^{jN2\pi d \sin\theta \cos\phi} \tag{4}$$

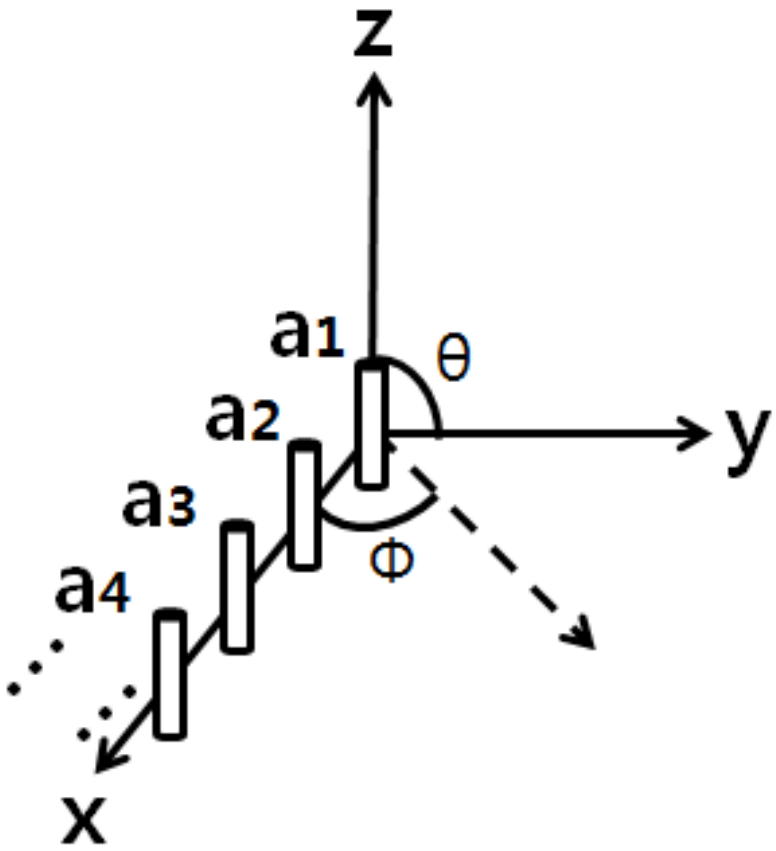

Figure 27 Linear array antenna elements' displacements in xyz coordinate

5.1.1 Assumptions

We assume that the transmitter and receiver have the same height; the elevation pattern will not greatly impact performance under this assumption, and can be ignored. Thus, we can align elements for a linear array antenna on the x-axis as shown in Figure 27. Also, we will be interested only in the azimuth beam pattern, plotted in the x-y plane; therefore, we consider $\Theta=90^\circ$ and only the value of ϕ will change. When we are deriving each element's weights, there are several parameters we can control, such as a distance between each element, *d*, and a number of elements, *N*. The parameters *d* and *N* will be

known and will have fixed values. The pattern will be synthesized by the weights that we derive. We consider that the linear array antenna will be mounted on top of a vehicle and used only for the OBU transmitter; the RSU will use an omnidirectional antenna as the receiver antenna.

Assumption 1: altitudes of transmitter and receiver are the same; effects due to the vertical pattern will be negligible.
Assumption 2: main beamforming pattern will be controlled in the x-y plane with a narrow vertical pattern. (Θ=90°, ϕ=0°)

Based on *Assumption 2*, in array factor, $A(\Theta,\phi)$, the terms that include Θ can be simplified because sin(90°) = 1. Therefore, the array factor can be simplified to $A(\phi)$, which can be represented and rewritten from (4) as:

$$A(\phi) = a_1 e^{j2\pi d \cos\phi} + a_2 e^{j2\cdot 2\pi d \cos\phi} + \cdots + a_N e^{jN2\pi d \cos\phi}$$
$$= \sum_{n=1}^{N} a_n e^{jn2\pi \cos\phi} \quad (5)$$

In (5), a_n represents each element's weight. Equation (5) is the initial setup for deriving a linear array antenna beamforming pattern based on GPS location of radios.

5.1.2 Interested Parameters

There are three parameters that we need to get from analysis based on GPS location of radios: Half-Power Beam-Width (HPBW), Beamwidth between first nulls (BWFN), and angle of maximum power gain. The angle of maximum power gain and the HPBW should be defined to cover the receivers to the left and to the right of the transmitter. But BWFN is more flexible than the other parameters; it is used for the variable to generate

beam pattern. The most important parameters are the angle of maximum power gain and HPBW. HPBW is the angle between the points where the main beam of power equals to one-half the maximum value [38]. BWFN is the angle between the points when power gain equals to Null, considered here as -40dB relative to maximum power [38]. As shown in Figure 28, ϕ_1 represents HPBW, ϕ_2 represents BWFN, and ϕ_{max} represents the angle of maximum gain. Based on GPS location of radios, we can find the angles for HPBW, BWFN, and ϕ_{max}. We will estimate weights of elements to satisfy the beam pattern of linear array antenna that has these parameters.

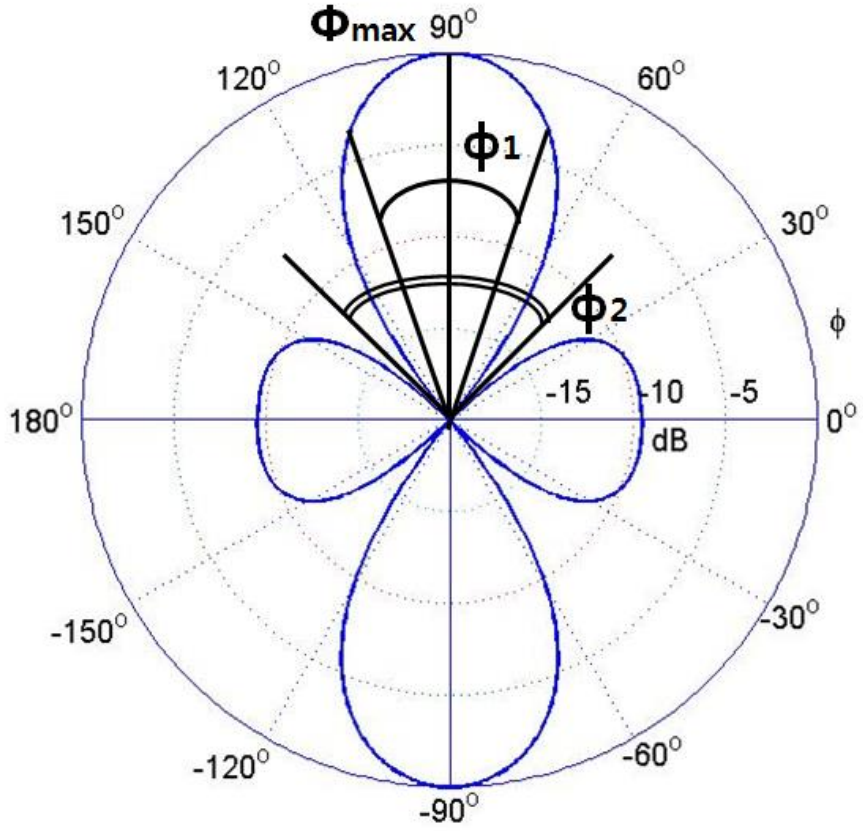

Figure 28 Angles of interest for beamforming pattern

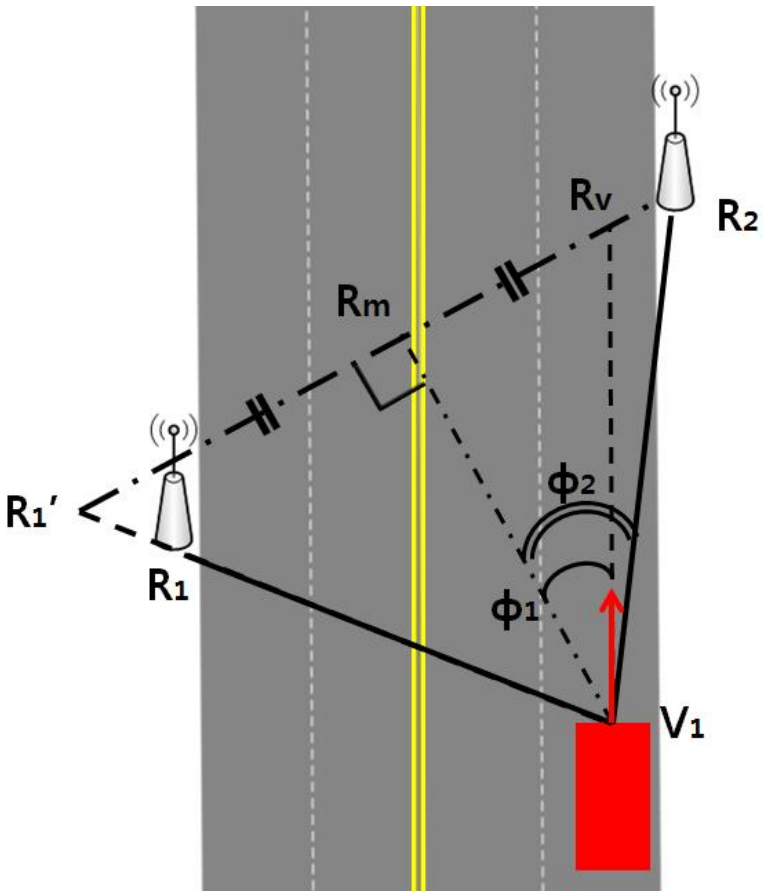

Figure 29 Desired angle calculation based on GPS location of nodes

5.1.2 Calculation based on GPS location

Since V2I communication has one fixed node and one moving node, if some application such as navigation can gather information of fixed node, the calculation to find out angles that antenna beam pattern needs to satisfy can be generated. The scenario for V2I communication is that a vehicle tends to transmit a signal to the fixed RSU as shown in Figure 29. As shown in Figure 29, the moving vehicle, V_1, two RSUs, R_1 and R_2, are the elements for V2I communication.

First, we need to find out the distance between the vehicle's OBU node the and RSU nodes. We set distance between R_1 and V_1 as d_1 and distance between R_2 and V_1 as d_2, and

then find out which distance is longer. Next, find the point which location is far from V_1 with same as longer distance but extended from shorter one; for Figure 29 case, d_1 is shorter, so we find new point R_1' which is located distance d_2 from V_1. Last, find the mid-point, R_m, of $\overline{R_1'R_2}$ and the point, R_v, which is the meeting point between $\overline{R_1'R_2}$ and projected line from V_1.

As shown in Figure 29, Φ_1 is the angle between $\overline{R_mV_1}$ and $\overline{R_vV_1}$ which represents the angle of the steering angle of beamforming pattern. Φ_2 is the angle between $\overline{R_mV_1}$ and $\overline{R_2V_1}$. Since $\Delta R_1'V_1R_2$ is an isosceles triangle, $2\Phi_2$ can be defined as the HPBW angle. We tried to find weights of linear array antenna elements to satisfy knowing variables Φ_1 and $2\Phi_2$.

Array steering is rotating the main lobe to a certain angle without physically changing the angle of the antenna [39]. The desired steering angle value is Φ_1, as shown in Figure 29. For representing array steering in equation form, (5) should be extended with steering phase which is represented as:

$$\psi_0 = 2\pi d \cos\phi_0 \tag{6}$$

In (6), Φ_0 is the steered angle which will be the same value as Φ_1. With steered angle, (5) can rewrite as:

$$A'(\psi) = A(\psi - \psi_0) = \sum_{n=1}^{N} a_n e^{jn2\pi\cos(\phi-\phi_0)} \tag{7}$$

The exponential term can be rewritten as weight portion and variable portion:

$$A'(\psi) = \sum_{n=1}^{N} a_n e^{-jn2\pi\cos\phi_0} e^{jn2\pi\cos\phi} \tag{8}$$

The form of a weight of element will be the term that contains variables a_n and ϕ_0 as shown in (8). Figure 29 shows the case of ϕ_0=30°.

Power gain is represented as the power that antenna beamforming generated in terms of ϕ [39]. Power gain can be represented as:

$$g(\phi) = \left|A(\phi)\right|^2 \tag{9}$$

For estimating weights, a_n, we need to set all the other parameters as fixed values, constant. Equation (9) with constant values, C_n, can be rewritten as:

$$g(\phi_i) = \left| a_1 e^{j2\pi d \cos(\phi_i - \phi_0)} + a_2 e^{j2 \cdot 2\pi d \cos(\phi_i - \phi_0)} + \cdots + a_N e^{jN2\pi d \cos(\phi_i - \phi_0)} \right|^2 \tag{10}$$
$$= \left|C_1 a_1 + C_2 a_2 + \cdots + C_N a_N\right|^2$$

Since the exponential terms, C_n, contains real, x_n, and imaginary, y_n, numbers, (10) can be rewritten as:

$$g(\phi_i) = \left|(x_1 + iy_1)a_1 + (x_2 + iy_2)a_2 + \cdots + (x_N + iy_N)a_N\right|^2 \tag{11}$$

(11) can be simplified to:

$$g(\phi_i) = (x_1 a_1 + x_2 a_2 + \cdots + x_N a_N)^2 - (y_1 a_1 + y_2 a_2 + \cdots + y_N a_N)^2$$
$$= \sum_{n=1}^{N} (x_n{}^2 - y_n{}^2) a_n{}^2 + \sum_{n=1}^{N-1} 2a_n \left\{ \sum_{m=n+1}^{N-1} \left(x_n x_m - y_n y_m\right) a_m \right\} \tag{12}$$

For estimating N number of elements' weight, N number of $g(\phi)$ and φ should be defined to apply in (12).

Our approach to finding a weight of each element for satisfying the desired beam pattern angles is:

1. Find ϕ_1 and $2\phi_2$ from GPS location of nodes
2. Apply ϕ_1 to (8) to find weight that impacts steering angle
3. Substitute *N* number of *g(*ϕ*)* and ϕ into (12)
4. By *N* numbers of (12)s, solve for a_n that satisfy the condition

5.2 Simulation

In this section, we set two realistic scenarios and parameters for beam pattern and proceed with our approach. Two scenarios and parameters are shown in Figure 30 and Table 6. Scenario A is the shorter distance between receivers and transmitter, and Scenario B is the longer distance. By the different distance, HPBW will be different as well as BWFN. Scenario A will have larger HPBW and more degree to steer than Scenario B.

Table 6. Parameters for Realistic Scenarios

	Scenario A	Scenario B
d1	50m	50m
d2	50m	300m
φ_1	22°	9.5°
$2\phi_2$	46°	20°
BWFN	27°	40°
N	5	5
d	0.495λ	0.5λ

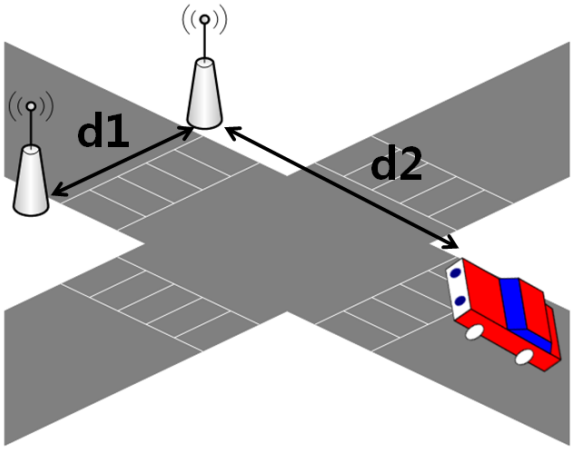

(a)

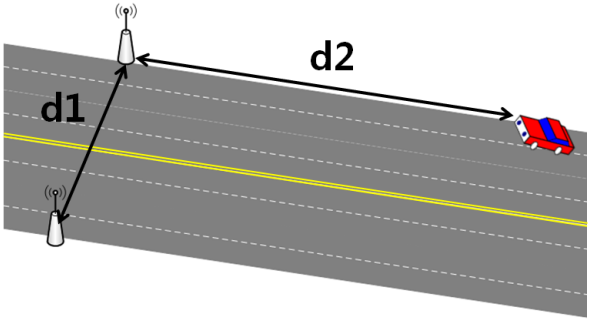

(b)

Figure 30 (a) Realistic scenario A (b) Realistic scenario B

With the parameters shown in Table 6, we were able to generate a beam pattern as shown with weights of each element in Table 7. The red line in Figure 31 is a marker of -3dB. Also, Figure 32 shows the beam pattern without steering to show whether the main lobe satisfies HPBW and the angle when gain is maximized.

As shown in Figure 31 (a), we were able to generate beam pattern with HPBW of approximately 46° and BWFN of 27°; even though there was some gain loss, about -2 ~ -3dB, at 90°, we can assume the main beam is centered at 90°. A definite null was not to generates at an exact angle; however, the beam is pointed at the desired angle and it is

assumed that the null could be generated similarly through use of a more detailed model of the element and array patterns. Also as shown in Figure 31 (a), the beam is steered to 22° from 90°. The weights for scenario A are shown in Table 7.

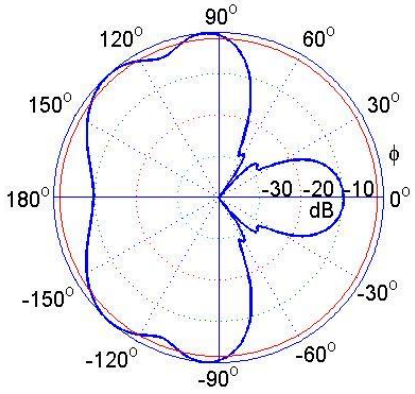

(a)

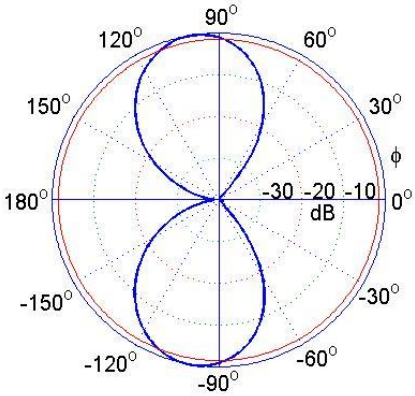

(b)

Figure 31 (a) Beam pattern for scenario A, (b) beam pattern for scenario B

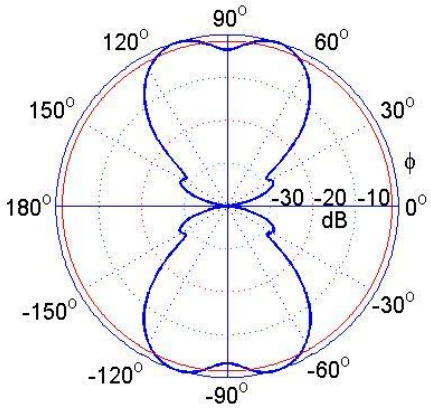

(a)

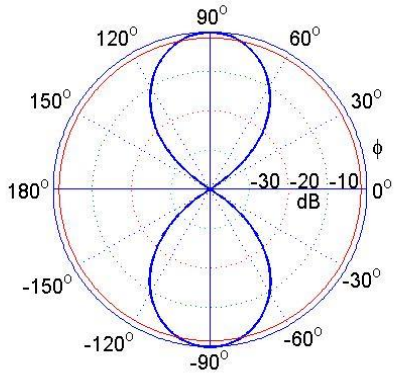

(b)

Figure 32 (a) Beam pattern w/o steering for scenario A, (b) beam pattern w/o steering for scenario B

As shown in Figure 32 (b), we were able to generate a beam pattern with HPBW of approximately 20°, BWFN of 40°, and max gain at 90°. Also as shown in Figure 31 (b), the beam is steered to 9.5° from 90°. The weights for scenario B are shown in Table 7.

By the results, our approach can find approximate weights for linear array antenna elements to satisfy the angle of maximum gain, HPBW, and BWFN which are found based on GPS locations of transmitter and receivers.

Since the study about mathematical approach for controllable array antenna is the first step of actual implementation of hardware, the objective is succeeded; the derived equation can be used to generate an approximation of the desired beam pattern. The next step of the research will be implementation of an actual hardware antenna with USRPs. We may face several problems due to the several assumptions that we made.

Table 7 Weights for Scenario A and Scenario B

	Scenario A		Scenario B	
Element	W/O Steering	With Steering	W/O Steering	With Steering
1	-33.95+0.05*i*	23.98+24.03*i*	17.33	8.82-14.92*i*
2	-25.69-0.06*i*	-9.92+23.70*i*	61.99	53.84-30.72*i*
3	57.72+0.05*i*	57.72+0.05*i*	75.47	75.47
4	90.24+0.02*i*	34.61+83.34*i*	34.26	29.76+16.98*i*
5	39.47-0.14*i*	-27.74+28.08*i*	2.50+0.0006*i*	1.27+2.15*i*

Chapter 6. Conclusions, Discussion, and Future Work

5G communication systems will be standardized and deployed in the future. One 5G application, IoV, will be an important aspect of communication systems for vehicular communications and will target many types of V2X applications. To support safety-critical as well as routine V2X applications, 5G systems must be flexible and be able to adapt their parameters and thresholds to cover all V2X use cases, particularly those involving safety-critical warning services.

LTE and DSRC are two strong candidates for IoV and cooperative solutions can exploit the advantages of each. Therefore, performance analysis of LTE and DSRC has focused especially end-to-end latency and system reliability, which are critical metrics for safety-critical V2X warning. Also, the radios for IoV are likely using an omnidirectional antenna; however, vehicles are moving continuously through locations and traffic configurations that present different propagation environments. To improve the efficiency of communication, the radios need to use flexible directional antennas such as a linear array with pattern synthesis and increase performance through a dynamic antenna. For example, in a propagation environment which contains high fading, under the assumption of Line-Of-Sight communication, a directional antenna will perform better than an omnidirectional antenna; however, in some fading environments, diversity combining using omnidirectional antennas, (omni-diversity) may perform better than a directional antenna.

We have analyzed the latency of LTE and DSRC with varying population of users, transmission priorities, system bandwidths, and cell radii. The DSRC results have shown

that distance has little effect on latency. A higher user priority, on the other hand, can improve the latency. Moreover, the latency of DSRC does not significantly increase when the population of the network increases. The LTE results showed that a wider system bandwidth and smaller cell radius significantly reduce the latency figure. Since LTE simulations are done with the scenario of VoIP, the latency results showed much larger value of latency than usual service of LTE, 4~5ms. The simulator can be improved with the availability of select real-life scenario, and the developed flexibility can aid to broader study of LTE service latency.

For warning applications that demand low latency, such as V2R and V2V, DSRC should use a higher priority, but LTE has some flexibility because, for small numbers of users per cell, its performance is similar, or even better than that of DSRC. For V2P and broadcast services that target a large number of users, LTE should use wider bandwidth and smaller cell radius whereas DSRC can use different parameter combinations since they have little effect on latency for large network populations.

From the results in Figure 31, Figure 32, and Table 7, the approach can find weights to achieve given beam pattern parameters that are found based on GPS locations of transmitter and receivers. Also, the beam pattern generated by the found weights satisfies the given beam pattern parameters. By the approach, the controllable linear array antenna can generate a beam pattern based on knowledge of its location and surroundings.

Although not fully considered in this analysis, array element weights also depend on mutual coupling between the elements. Mutual coupling is implementation-specific since it varies with several factors including array configuration, element spacing, and element

orientation. A full implementation of the array must take this into consideration during the design process.

Some limitations exist. It is not possible to generate all desired combinations of HPBW and BWFN. Also for certain high or low values of HPBW and BWFN, it was not possible to generate clean beam patterns as shown in Figure 32 (b). Characterization of the relationship between a number of elements, HPBW, and BWFN is planned. Also, in future research including hardware implementation, effects of mutual coupling, which was not considered in this analysis, should be considered. In addition, other array geometries, such as circular arrays, may be considered.

V2X must flexibly cover all existing vehicle-related communication systems, and the standard for V2X, possibly including LTE and DSRC cooperation, must include functions and controllable parameters such as channel scheduling, signal bandwidth, transmit power, packet structure, and network size. This and future studies of performance that explore effects of varying the different parameters will guide flexible adoption of technologies for 5G services in a variety of scenarios that have distinct requirements.

Reference

[1] G. I. P. P. Partnership, "5G Vision," February, 2015.

[2] J. G. Andrews, S. Buzzi, W. Choi, S. V. Hanly, A. Lozano, A. C. Soong, *et al*., "What will 5G be?," *Selected Areas in Communications, IEEE Journal on*, vol. 32, pp. 1065-1082, 2014.

[3] H. Moiin, "Looking ahead to 5G – A symbiotic convergence of new and existing technologies," presented at the EUCNC, 2014.

[4] J. Morrish. (June 2013). *The Connected Life*. Available: www.gsma.com

[5] B. C. Cheng *et al*., "Survey on networking for Internet of Vehicles," *J. Internet Technol.*, vol. 14, no. 7, pp. 1007-1020, Dec. 2013.

[6] N. H. T. S. Administration, "Safety in Numbers," vol. Volume 1 Issue 4, ed, August 2013.

[7] N. H. T. S. Administration, "Traffic Safety Facts, 2012 Data: Pedestrian," *Annals of Emergency Medicine*, vol. 65, p. 452, 2015.

[8] Federal Railroad Administration – Office of Safety Analysis Databases. Available: http://safetydata.fra.dot.gov/OfficeofSafety/Default.aspx

[9] A. Vinel, "3GPP LTE versus IEEE 802.11 p/WAVE: which technology is able to support cooperative vehicular safety applications?," *Wireless Communications Letters, IEEE*, vol. 1, pp. 125-128, 2012.

[10] S. Kato, M. Hiltune, K. Joshi, and R. Schlichting, "Enabling vehicular safety applications over LTE networks," in *Connected Vehicles and Expo (ICCVE), 2013 International Conference on*, 2013, pp. 747-752.

[11] L. Gallo and J. Harri, "Short paper: A LTE-direct broadcast mechanism for periodic vehicular safety communications," in *Vehicular Networking Conference (VNC),2013 IEEE*, 2013, pp. 166-169.

[12] Z. H. Mir and F. Filali, "LTE and IEEE 802.11 p for vehicular networking: a performance evaluation," *EURASIP Journal on Wireless Communications and Networking*, vol. 2014, pp. 1-15, 2014.

[13] K. Trichias, v. d. J. Berg, G. Heijenk, d. J. Jongh, and R. Litjens, "Modeling and evaluation of LTE in intelligent transportation systems," 2012.

[14] G. Araniti, C. Campolo, M. Condoluci, A. Iera, and A. Molinaro, "LTE for vehicular networking: a survey," *Communications Magazine, IEEE*, vol. 51, pp. 148-157, 2013.

[15] H. Onishi and F. Mlinarsky, "Wireless technology assessment for automotive applications," in *Proc. ITS World Congress*, 2012.

[16] R. Atat, E. Yaacoub, M. S. Alouini, and F. Filali, "Delay efficient cooperation in public safety vehicular networks using LTE and IEEE 802.11 p," in *Consumer Communications and Networking Conference (CCNC), 2012 IEEE*, 2012, pp. 316-320.

[17] P. Caballero-Gil, C. Caballero-Gil, and J. Molina-Gil, "Design and implementation of an application for deploying vehicular networks with smartphones," *International Journal of Distributed Sensor Networks*, vol. 2013, 2013.

[18] S. Tornell, C. T. Calafate, J. C. Cano, P. Manzoni, M. Fogue, and F. J. Martinez, "Evaluating the feasibility of using smartphones for ITS safety applications," in *Vehicular Technology Conference (VTC Spring), 2013 IEEE 77th*, 2013, pp. 1-5.

[19] J. J. Anaya, P. Merdrigna, O. Shagdar, F. Nashashibi, and J. E. Naranjo, "Vehicle to pedestrian communications for protection of vulnerable road users," in *Intelligent Vehicles Symposium Proceedings, 2014 IEEE*, 2014, pp. 1037-1042.

[20] *Honda Demonstrates Advanced Vehicle-to-Pedestrian and Vehicle-to-Motorcycle Safety Technologies* Available: http://www.prnewswire.com/news-releases/honda-demonstrates-advanced-vehicle-to-pedestrian-and-vehicle-to-motorcycle-safety-technologies-221495031.html

[21] Y. S. Song, J. Kim, S. W. Choi, and Y. K. Kim, "Long term evolution for wireless railway communications: testbed deployment and performance evaluation," *IEEE Communications Magazine*, Vol. 54, Iss. 2, pp. 138-145, Feb. 2016.

[22] S. Ucar, S. C. Ergen, and O. Ozkasap, "Multihop-cluster-based IEEE 802.11p and LTE hybrid architecture for VANET safety message dissemination," *IEEE Trans. Veh. Techn.*, Vol 65, Iss. 4, pp. 2621-2636, April 2016.

[23] A. Mostafa, A. M. Vegni, R. Singoria, T. Oliveira, T. D. Little, and D. P. Agrawal, "A V2X-based approach for reduction of delay propagation in vehicular Ad-hoc networks," in *ITS Telecommunications (ITST), 2011 11th*

International Conference on 2011, pp. 756-761.

[24] L. Reggiani, L. Dossi, L. G. Giordano, and R. Lambiase, *Small LTE Base Stations Deployment in Vehicle-to-Road-Infrastructure Communications:* INTECH Open Access Publisher, 2013.

[25] E. Abd-Elrahman, A. M. Said, T. Toukabri, H. Afifi, and M. Marot, "Assisting V2V failure recovery using Device-to-Device Communications," in *Wireless Days (WD), 2014 IFIP*, 2014, pp. 1-3.

[26] G. Hattori, C. Ono, S. Nishiyama, and H. Horiuchi, "Implementation and evaluation of message delegation middleware for its application," in *Applications and the Internet Workshops, 2004, SAINT 2004 Workshops. 2004 International Symposium on*, 2004, pp. 326-333.

[27] A. Elmurtada, Y. Awad, and M. Elnourani, "Adaptive Smart Antennas in 3G Networks and Beyond," in *Research and Development (SCORed) IEEE Student Conference 2012*, pp. 148-153.

[28] S. Pyun, H. Widiarti, and Y. Kwon, "Group-Based Channel Access Scheme for a V2I Communication System using Smart Antenna," *IEEE Communications Letters*, no. 8 (2011), pp. 804-806.

[29] H. Wu, C. Liu, and Y. Dai, "Adaptive Pattern Nulling Design of Linear Array Antenna by Phase Perturbations Using Invasive Weed Optimization Algorithm," in *2013 IEEE Third International Conference on Information Science and Technology (ICIST)*. 2013.

[30] X. Z. D. Qiao, "Quality, Reliability, Securit and Robustness in Heterogeneous Networks."

[31] W. Vandenberghs, I. Moerman, and P. Demeester, "Approximation of the IEEE 802.11 p standard using commercial off-the-shelf IEEE 802.11 a hardware," in *ITE Telecommunications (ITST), 2011 11th International Conference on*, 2011, pp. 21-26.

[32] L. M. s. Committee, "Part 11: Wireless lan medium access control (mac) and physical layer (phy) specifications," *IEEE-SA Standards Board*, 2003.

[33] *IEEE 802.11a WLAN Physical Layer, MathWorks*, Available: http://www.mathworks.com/help/releases/R2015b/comm/examples/ieee-802-11a-wlan-physical-layer.html

[34] J. Choi, S. Guha, C. B. Dietrich, "A Simulink-based Model and Analysis of the PHY Layer in Vehicular Communications," presented at the WInnComm 2015,

San Diego, CA, 2015.

[35] E. N. Committee, Channel models for HIPERLAN/2 in different indoor scenarios," *Norme ETSI, document 3ERI085B, European Telecommunications Standards Institute, Sophia-Antipolis, Valbonne, France, 1998.*

[36] A. Doufexi, S. Armour, M. Butler, An. Nix, D. Bull, J. McGeehan, *et al*., "A comparison of the HIPERLAN/2 and IEEE 802.11 a wireless LAN standards," *Communications Magazine, IEEE*, vol. 40, pp. 172-180, 2002.

[37] *SimuLTE*. Available: http://simulte.com/

[38] W. Stutzman and G. Thiele, "Antenna Theory and Design," 2nd ed. 1998.

[39] S. Orfanidis, "Electromagnetic Waves and Antennas," 2016. Available: http://www.ece.rutgers.edu/~orfanidi/ewa/

Appendix A

HIPERLAN/2 Model C

Tap Number	Delay (ns)	Average Relative Power (dB)	Ricean K	Doppler Spectrum
1	0	-3.3	0	Class
2	10	-3.6	0	Class
3	20	-3.9	0	Class
4	30	-4.2	0	Class
5	50	0.0	0	Class
6	80	-0.9	0	Class
7	110	-1.7	0	Class
8	140	-2.6	0	Class
9	180	-1.5	0	Class
10	230	-3.0	0	Class
11	280	-4.4	0	Class
12	330	-5.9	0	Class
13	400	-5.3	0	Class
14	490	-7.9	0	Class
15	600	-9.4	0	Class
16	730	-13.2	0	Class
17	880	-16.3	0	Class
18	1050	-21.2	0	Class

Appendix B

DSRC PHY Performance

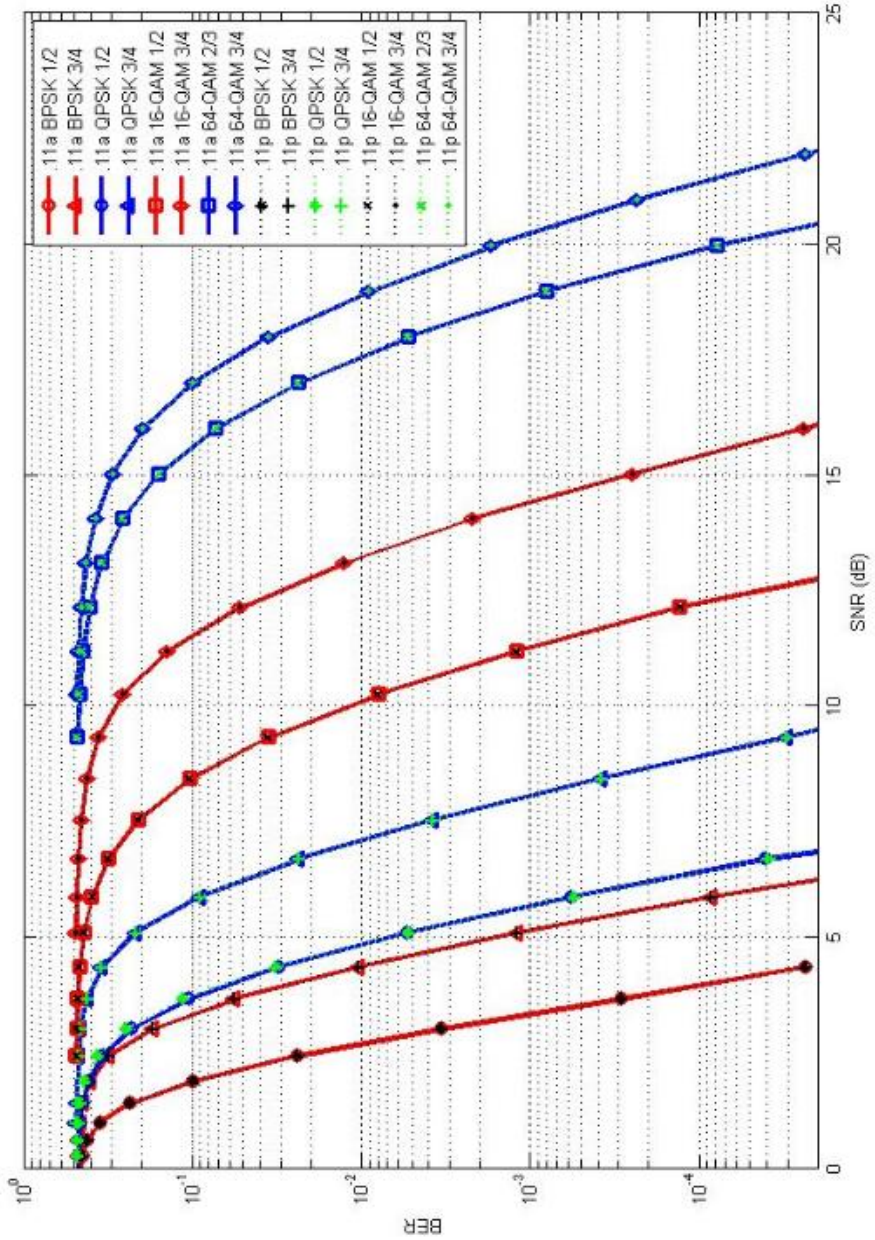

Figure 33 Validation: Comparison between IEEE 802.11a and IEEE 802.11p in AWGN

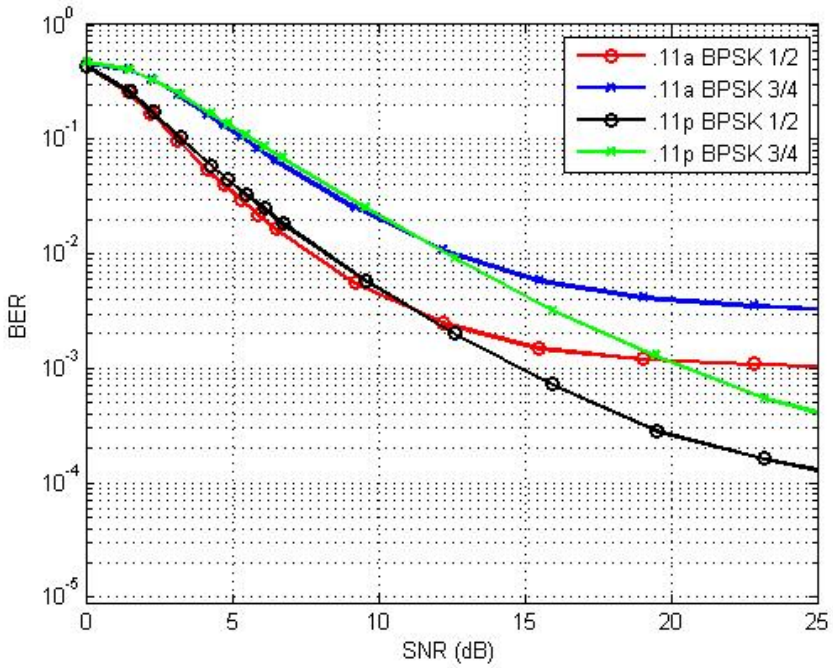

Figure 34 Comparison between IEEE 802.11a and IEEE 802.11p in Rayleigh Fading

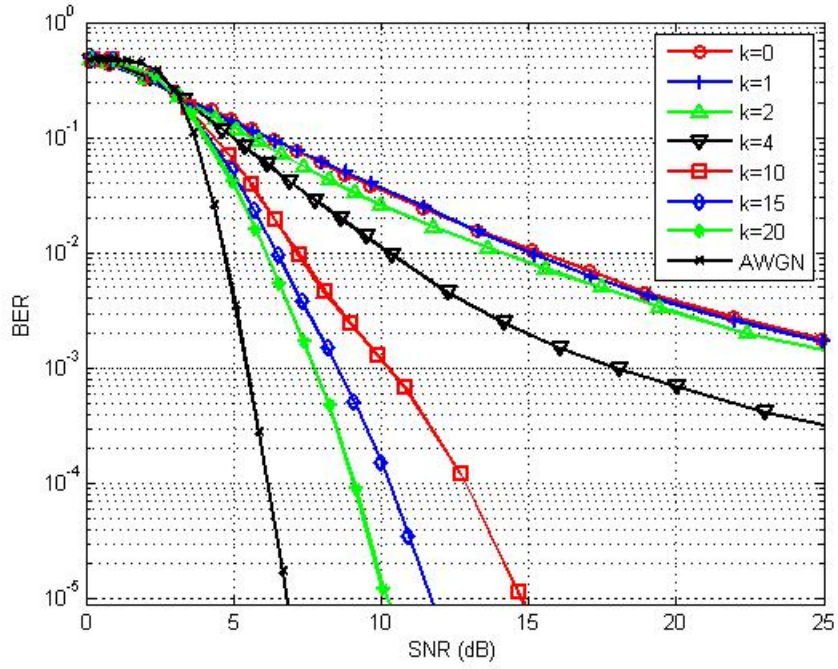

Figure 35 IEEE 802.11p Performance in Rayleigh and Rician Fading

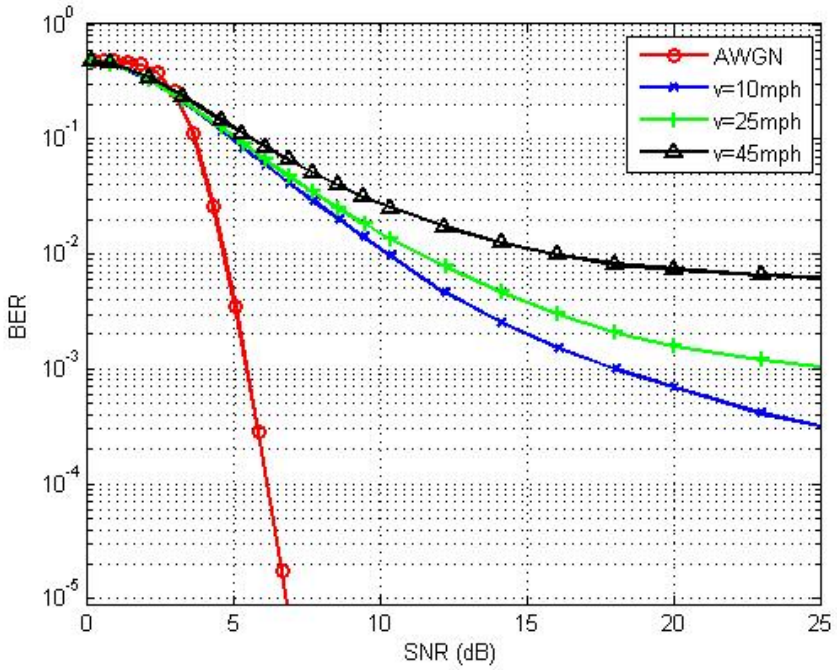

Figure 36 Effect of velocity on 802.11p (Rician Fading k=4)

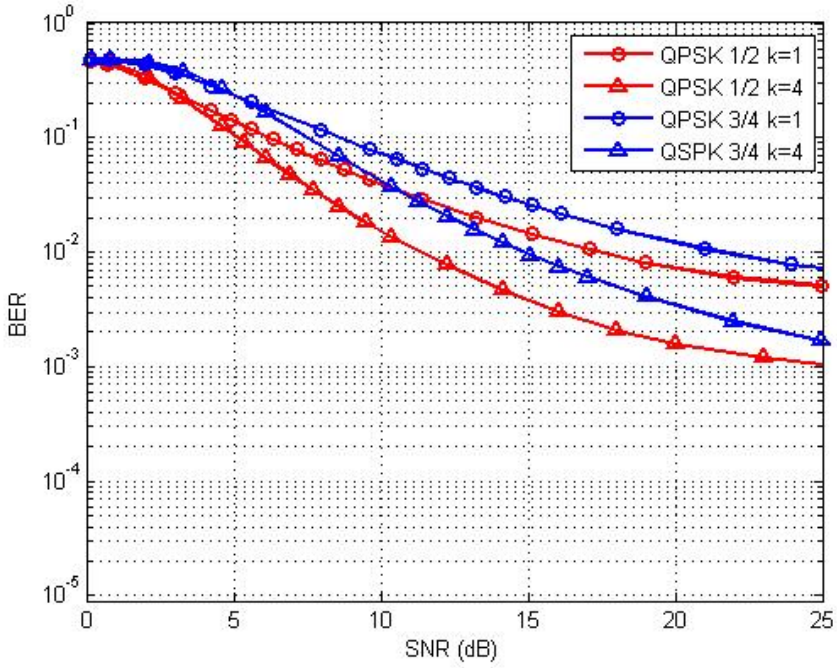

Figure 37 Effect of coding rate on 802.11p (Rician Fading v=25mph)

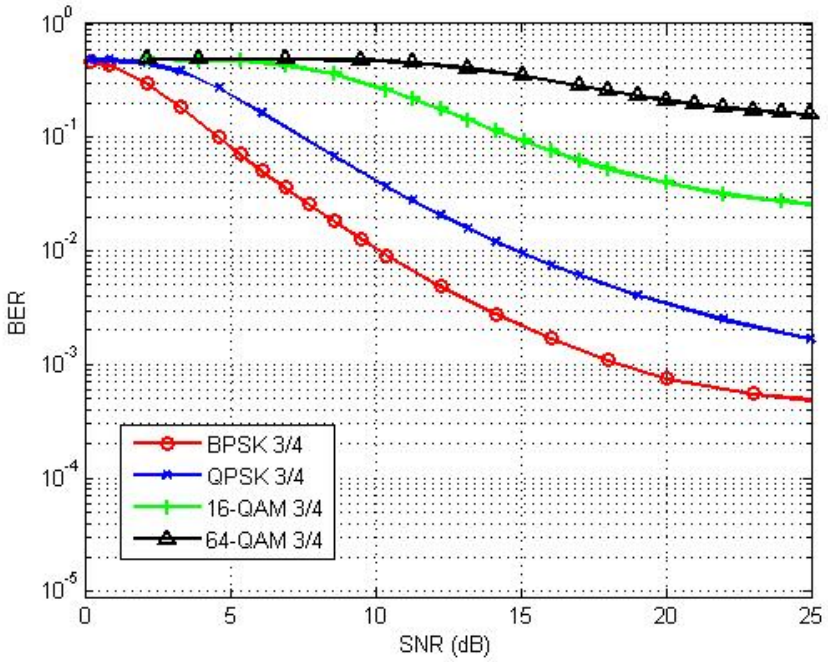

Figure 38 Effect of Modulation Schemes (Rician Fading k=4 v=25mph)

Appendix C

CSMA/CD Protocol Matlab Script

```
%%%%%%%%%%%%%%%%%%%%%%%%%%%%%%%% CSMA protocol%%%

 % State - 0

transition_0to1 = zeros(1,n);
to_send = rand(1,n);

transition_0to1(state == 0 & to_send < traffic ) = 1;

temp_vec = sifs + rand(1,n) * 2 * fsize;
frame_length(state ==0 & transition_0to1 > 0) = temp_vec(state ==0 & transition_0to1 > 0);

temp_vec = ceil(rand(1,n) * n);
frame_dest(state == 0 & transition_0to1 > 0)  = temp_vec(state ==0 & transition_0to1 > 0);

for i = 1:n
    while ( frame_dest(i) == i | frame_dest(i) == 0)
        frame_dest(i) = ceil(rand * n);
    end
end

temp_vec = floor(rand(1,n) .* (2.^CW));
BCounter(state == 0 & transition_0to1 > 0) = temp_vec(state == 0 & transition_0to1 > 0) * slot_time;

state(transition_0to1 > 0) = 1;

%%%%%%%%%%%%%%%%%%%%%%%%%%%%%%%%%%%%%%%%%%%%%%

 % State - 1

% Medium Sensing
 sending = zeros(1,n);
 sending(state <= -1 | state >= 5) = 1;
 %sending
 busy_medium = sending * distance_matrix;

 transition_1to2 = zeros(1,n);
 transition_1to2(state == 1 & busy_medium < 1) = 1;
 for g = 1:n
     if (state(g) == 1 & busy_medium <1)
         p(g) = p(g)+1;
         delay(g,p(g)) = delay_counter (g);
         delay_counter(g) = 0;
     end
     if (state(g) == 1 & busy_medium == 1)
         delay_counter(g) = delay_counter(g)+1;
     end
 end


 %%%%%%%%%%%%%%%%%%%%%%%%%%%%%%%%%%%%%%%%%%%%%%

 % State - 2
 % Difs Timer

 timer(transition_1to2 > 0) = difs;
 transition_2to1 = zeros(1,n);
 transition_2to1(state == 2 & busy_medium > 0) = 1;

 timer(state == 2) = timer(state == 2) - 1;
 delay_counter(state == 2) = delay_counter(state == 2) + 1;

 transition_2to3 = zeros(1,n);
 transition_2to3(state == 2 & timer<0) = 1;

 %%%%%%%%%%%%%%%%%%%%%%%%%%%%%%%%%%%%%%%%%%%%%%
```

```
% State - 3

BCounter(state == 3 & busy_medium < 1) =  BCounter(state == 3 & busy_medium < 1) - 1;
delay_counter(state == 3) =  delay_counter(state == 3) + 1;

transition_3to5 = zeros(1,n);
transition_3to5(state == 3 & BCounter<0) = 1;

%%%%%%%%%%%%%%%%%%%%%%%%%%%%%%%%%%%%%%%%%%%%%%%%%%%%
temp_rand = rand (1,n);
% State - 5

for i = 1:n

    if (state(i) == 5 & busy_medium(frame_dest(i)) > 1)

        state(i) = 6;
        delay_counter (i) = delay_counter(i) + 1;
    end

    if (state(i) == 5 & temp_rand < PER(i,frame_dest(i))) %%This ensures that a PER% of packets are lost.

        state(i) = 7; %%State = 7 -> Packet lost due to low SNR
        delay_counter (i) = delay_counter(i) + 1;
    end

end

frame_length(state >= 5) = frame_length(state >= 5) - 1;
%%delay_counter(state >= 5) = delay_counter(state >= 5) + 1;

transition_5to0 = zeros(1,n);
transition_5to0(state >=5 & frame_length < 0) = 1;

CW(state > 5 & transition_5to0 > 0) = CW(state > 5 & transition_5to0 > 0) + 1;
CW(CW > CWmax) = CWmax;
CW(state == 5 & transition_5to0 > 0) = CWmin;

total_transmissions(r) = total_transmissions(r) +
                         length(state(state >= 5 & transition_5to0 > 0));  %% Total Number of transmissions

successful_transmission(r) = successful_transmission(r) +
                             length(state(state == 5 & transition_5to0 >0)); %% Transmissions that were successfully received
total_collisions = total_collisions + length(state(state == 6 & transition_5to0 > 0)); %% Collisions

unreachable_packets = unreachable_packets +
                      length(state(state == 7 & transition_5to0 > 0)); %% Packets whose SNR was too low at the receiver

transition_5to4 = zeros(1,n);

for i = 1:n
    if(state(i) == 5 & transition_5to0(i) > 0)

        transition_5to4(frame_dest(i)) = 1;
        timer(frame_dest(i)) = sifs;
        ack_dest(frame_dest(i)) = i;

    end
end

%state(transition_5to4 > 0) = 4;
timer(state == 4 & busy_medium > 0) = sifs;

timer(state == 4 & busy_medium < 1) = timer(state == 4 & busy_medium < 1) - 1;

%timer(state == 4) = timer(state == 4) - 1


transition_4to1 = zeros(1,n);
transition_4to1(state == 4 & timer < 0) = 1;
timer(transition_4to1 > 0) = ack_length;
```

```
%%%%%%%%%%%%%%%%%%%%%%%%%%%%%%%%%%%%%%%%%%%%%%%%%%%%

% State - -1

for i = 1:n


    if (state(i) == -1 && busy_medium(ack_dest(i)) > 1)

        state(i) = -2;

    end

    %%if (state(i) == -1 && distance_matrix(i,ack_dest(i)) < 1)
    if (state(i) == -1 & temp_rand < PER(i,ack_dest(i)))
        state(i) = -3;

    end



end

timer(state <= -1) = timer(state <= -1) - 1;

transition_m1to0 = zeros(1,n);
transition_m1to0(state <= -1 & timer < 0) = 1;

total_acks = total_acks + length(state(state <= -1 & transition_m1to0 > 0));
successful_acks = successful_acks + length(state(state == -1 & transition_m1to0 > 0));
ack_collisions = ack_collisions + length(state(state == -2 & transition_m1to0 > 0));
unreachable_acks = unreachable_acks + length(state(state == -3 & transition_m1to0 > 0));

%state
%%%%%%%%%%%%%%%%%%%%%%%%%%%%%%%%%%%%%%%%%%%%%%%%%%%%
% States Conversion

state(transition_0to1 > 0)  =  1;
state(transition_1to2 > 0)  =  2;
state(transition_2to3 > 0)  =  3;
state(transition_3to5 > 0)  =  5;
state(transition_2to1 > 0)  =  1;
state(transition_5to0 > 0)  =  0;
state(transition_5to4 > 0)  =  4;
state(transition_4tom1 > 0) = -1;
state(transition_m1to0 > 0) =  0;

i;
state;
delay_counter;

delay(i) = delay_counter(1);

%state
```

Appendix D

SimuLTE Parameter Control Window

Section/Key	Value	Comment
Config SingleCell-DL		
*.ue[*].udpApp[0].typename	"VoIPReceiver"	
*.server.udpApp[*].destAddress	"ue["+string(ancestorI...	obtain the ...
*.server.udpApp[*].localPort	3088+ancestorIndex(0)	
*.server.udpApp[*].typename	"VoIPSender"	
*.server.udpApp[*].startTime	uniform(0s,0.02s)	
Config SingleCell		
*.numUe	${numUEs=50}	
*.ue[*].numUdpApps	1	
*.server.numUdpApps	${numUEs}	application...
**.ue[*].macCellId	1	
**.ue[*].masterId	1	
*.eNodeB.mobility.initFromDisplayString	false	
*.eNodeB.mobility.initialX	300m	
*.eNodeB.mobility.initialY	300m	
*.ue[*].mobility.constraintAreaMaxX	818m	
*.ue[*].mobility.constraintAreaMaxY	599m	
*.ue[*].mobility.constraintAreaMinX	-218m	
*.ue[*].mobility.constraintAreaMinY	1m	
*.ue[*].mobility.initFromDisplayString	false	
*.ue[*].mobility.initialX	uniform(-218m,818m)	
*.ue[*].mobility.initialY	uniform(1m,599m)	
*.ue[*].mobility.speed	1mps	
*.ue[*].mobilityType	"LinearMobility"	
General		
**.channelControl.pMax	5W	
**.channelControl.alpha	1.0	
**.channelControl.carrierFrequency	2100e+6Hz	
**.nic.phy.channelModel	xmldoc("config_chann...	
**.feedbackComputation	xmldoc("config_chann...	
**.fbDelay	1	
**.mobility.constraintAreaMinZ	0m	
**.mobility.constraintAreaMaxZ	0m	
**.rbAllocationType	"localized"	
**.deployer.numRbDl	6	
**.deployer.numRbUl	6	
**.numBands	6	

SimuLTE Channel Configuration

```
<ChannelModel type="REAL">
        <!-- Enable/disable shadowing -->
    <parameter name="shadowing" type="bool" value="true"/>
    <!-- Pathloss scenario from ITU -->
    <parameter name="scenario" type="string" value="URBAN_MACROCELL"/>
    <!-- eNodeB height -->
    <parameter name="nodeb-height" type="double" value="25"/>
    <!-- ue height -->
    <parameter name="ue-height" type="double" value="1.5"/>
    <!-- Building height -->
    <parameter name="building-height" type="double" value="18"/>
    <!-- Carrier Frequency (GHz) -->
    <parameter name="carrierFrequency" type="double" value="2"/>
    <!-- Target bler used to compute feedback -->
    <parameter name="targetBler" type="double" value="0.001"/>
    <!-- HARQ reduction -->
    <parameter name="harqReduction" type="double" value="0.2"/>
    <!-- Rank indicator tracefile -->
    <parameter name="lambdaMinTh" type="double" value="0.02"/>
    <parameter name="lambdaMaxTh" type="double" value="0.2"/>
    <parameter name="lambdaRatioTh" type="double" value="20"/>
    <!-- Antenna Gain of UE -->
    <parameter name="antennaGainUe" type="double" value="0"/>
    <!-- Antenna Gain of eNodeB -->
    <parameter name="antennGainEnB" type="double" value="18"/>
    <!-- Antenna Gain of Micro node -->
    <parameter name="antennGainMicro" type="double" value="5"/>
                <!-- Thermal Noise for 10 MHz of Bandwidth -->
    <parameter name="thermalNoise" type="double" value="-104.5"/>
    <!-- Ue noise figure -->
    <parameter name="ue-noise-figure" type="double" value="7"/>
    <!-- eNodeB noise figure -->
    <parameter name="bs-noise-figure" type="double" value="5"/>
    <!-- Cable Loss -->
    <parameter name="cable-loss" type="double" value="2"/>
    <!-- If true enable the possibility to switch dinamically the LOS/NLOS pathloss computation -->
    <parameter name="dynamic-los" type="bool" value="false"/>
    <!-- If dynamic-los is false this parameter, if true, compute LOS pathloss otherwise compute NLOS pathloss -->
    <parameter name="fixed-los" type="bool" value="false"/>
    <!-- Enable/disable fading -->
    <parameter name="fading" type="bool" value="true"/>
    <!-- Fading type (JAKES or RAYGHLEY) -->
    <parameter name="fading-type" type="string" value="JAKES"/>
    <!-- If jakes fading this parameter specify the number of path (tap channel) -->
    <parameter name="fading-paths" type="int" value="6"/>
                <!-- if true, enables the inter-cell interference computation -->
    <parameter name="extCell-interference" type="bool" value="true"/>
                <!-- if true, enables the multi-cell interference computation -->
    <parameter name="multiCell-interference" type="bool" value="true"/>
</ChannelModel>

<!-- Feedback Type (REAL, DUMMY) -->
<FeedbackComputation type="REAL">
        <!-- Target bler used to compute feedback -->
        <parameter name="targetBler" type="double" value="0.001"/>
        <!-- Rank indicator tracefile -->
     <parameter name="lambdaMinTh" type="double" value="0.02"/>
     <parameter name="lambdaMaxTh" type="double" value="0.2"/>
     <parameter name="lambdaRatioTh" type="double" value="20"/>
</FeedbackComputation>
```

Appendix E

Finding Weights for 5 element Linear Array Antenna

```
clear all; close all; digits(4);

N = 5; %number of element
syms a b c d e f; %# of them are depends on N
dis = 0.5; %distance between each element

phi_max = 0; %max at phi = 90
phi_3dB = 60; %3dB Beamwidth
phi_Null = 17; %Null additional angle to 3dB BW

%Detail Angle Values will use for gain1d function
psi_3dB1 = phi_max-(phi_3dB)/2;
psi_3dB2 = phi_max+(phi_3dB)/2;
psi_Null1 = phi_max-(((phi_3dB)/2)+phi_Null);
psi_Null2 = phi_max+(((phi_3dB)/2)+phi_Null);

phi_degree = [phi_max psi_3dB1 psi_Null1 psi_3dB2 psi_Null2 95 85];
phi = phi_degree * pi / 180;
gaindB = [0 -3 -40 -3 -40 -1 -1];
gainmag = db2mag(gaindB);

AF1 = arrayfactor(phi(1),dis,1);
RA1 = real(AF1);
IA1 = imag(AF1);

AF2 = arrayfactor(phi(1),dis,2);
RA2 = real(AF2);
IA2 = imag(AF2);

AF3 = arrayfactor(phi(1),dis,3);
RA3 = real(AF3);
IA3 = imag(AF3);

AF4 = arrayfactor(phi(1),dis,4);
RA4 = real(AF4);
IA4 = imag(AF4);

AF5 = arrayfactor(phi(1),dis,5);
RA5 = real(AF5);
IA5 = imag(AF5);
```

```
AF6 = arrayfactor(phi(2),dis,1);
RA6 = real(AF6);
IA6 = imag(AF6);

AF7 = arrayfactor(phi(2),dis,2);
RA7 = real(AF7);
IA7 = imag(AF7);

AF8 = arrayfactor(phi(2),dis,3);
RA8 = real(AF8);
IA8 = imag(AF8);

AF9 = arrayfactor(phi(2),dis,4);
RA9 = real(AF9);
IA9 = imag(AF9);

AF10 = arrayfactor(phi(2),dis,5);
RA10 = real(AF10);
IA10 = imag(AF10);

AF11 = arrayfactor(phi(3),dis,1);
RA11 = real(AF11);
IA11 = imag(AF11);

AF12 = arrayfactor(phi(3),dis,2);
RA12 = real(AF12);
IA12 = imag(AF12);

AF13 = arrayfactor(phi(3),dis,3);
RA13 = real(AF13);
IA13 = imag(AF13);

AF14 = arrayfactor(phi(3),dis,4);
RA14 = real(AF14);
IA14 = imag(AF14);

AF15 = arrayfactor(phi(3),dis,5);
RA15 = real(AF15);
IA15 = imag(AF15);
```

```
AF16 = arrayfactor(phi(4),dis,1);
RA16 = real(AF16);
IA16 = imag(AF16);

AF17 = arrayfactor(phi(4),dis,2);
RA17 = real(AF17);
IA17 = imag(AF17);

AF18 = arrayfactor(phi(4),dis,3);
RA18 = real(AF18);
IA18 = imag(AF18);

AF19 = arrayfactor(phi(4),dis,4);
RA19 = real(AF19);
IA19 = imag(AF19);

AF20 = arrayfactor(phi(4),dis,5);
RA20 = real(AF20);
IA20 = imag(AF20);

AF21 = arrayfactor(phi(5),dis,1);
RA21 = real(AF21);
IA21 = imag(AF21);

AF22 = arrayfactor(phi(5),dis,2);
RA22 = real(AF22);
IA22 = imag(AF22);

AF23 = arrayfactor(phi(5),dis,3);
RA23 = real(AF23);
IA23 = imag(AF23);

AF24 = arrayfactor(phi(5),dis,4);
RA24 = real(AF24);
IA24 = imag(AF24);

AF25 = arrayfactor(phi(5),dis,5);
RA25 = real(AF25);
IA25 = imag(AF25);
```

```
g(1) = (RA1^2 - IA1^2) * a^2 + (RA2^2 - IA2^2) * b^2 + (RA3^2 - IA3^2) * c^2 + (RA4^2 - IA4^2) * d^2 + (RA5^2 - IA5^2) * e^2 + 2*(RA1*RA2 - IA1*IA2)*a*b
 + 2*(RA1*RA3 - IA1*IA3)*a*c + 2*(RA1*RA4 - IA1*IA4)*a*d + 2*(RA1*RA5 - IA1*IA5)*a*e + 2*(RA2*RA3 - IA2*IA3)*b*c + 2*(RA2*RA4 - IA2*IA4)*b*d
 + 2*(RA2*RA5 - IA2*IA5)*b*e + 2*(RA3*RA4 - IA3*IA4)*c*d + 2*(RA3*RA5 - IA3*IA5)*c*e + 2*(RA4*RA5 - IA4*IA5)*d*e;

g(2) = (RA6^2 - IA6^2) * a^2 + (RA7^2 - IA7^2) * b^2 + (RA8^2 - IA8^2) * c^2 + (RA9^2 - IA9^2) * d^2 + (RA10^2 - IA10^2) * e^2 + 2*(RA6*RA7 - IA6*IA7)*a*b
 + 2*(RA6*RA8 - IA6*IA8)*a*c + 2*(RA6*RA9 - IA6*IA9)*a*d + 2*(RA6*RA10 - IA6*IA10)*a*e + 2*(RA7*RA8 - IA7*IA8)*b*c + 2*(RA7*RA9 - IA7*IA9)*b*d + 2*(RA7*RA10 - IA7*IA10)*b*e
 + 2*(RA8*RA9 - IA8*IA9)*c*d + 2*(RA8*RA10 - IA8*IA10)*c*e + 2*(RA9*RA10 - IA9*IA10)*d*e;

g(3) = (RA11^2 - IA11^2) * a^2 + (RA12^2 - IA12^2) * b^2 + (RA13^2 - IA13^2) * c^2 + (RA14^2 - IA14^2) * d^2 + (RA15^2 - IA15^2) * e^2 + 2*(RA11*RA12 - IA11*IA12)*a*b
 + 2*(RA11*RA13 - IA11*IA13)*a*c + 2*(RA11*RA14 - IA11*IA14)*a*d + 2*(RA11*RA15 - IA11*IA15)*a*e + 2*(RA12*RA13 - IA12*IA13)*b*c + 2*(RA12*RA14 - IA12*IA14)*b*d
 + 2*(RA12*RA15 - IA12*IA15)*b*e + 2*(RA13*RA14 - IA13*IA14)*c*d + 2*(RA13*RA15 - IA13*IA15)*c*e + 2*(RA14*RA15 - IA14*IA15)*d*e;

g(4) = (RA16^2 - IA16^2) * a^2 + (RA17^2 - IA17^2) * b^2 + (RA18^2 - IA18^2) * c^2 + (RA19^2 - IA19^2) * d^2 + (RA20^2 - IA20^2) * e^2 + 2*(RA16*RA17 - IA16*IA17)*a*b
 + 2*(RA16*RA18 - IA16*IA18)*a*c + 2*(RA16*RA19 - IA16*IA19)*a*d + 2*(RA16*RA20 - IA16*IA20)*a*e + 2*(RA17*RA18 - IA17*IA18)*b*c + 2*(RA17*RA19 - IA17*IA19)*b*d
 + 2*(RA17*RA20 - IA17*IA20)*b*e + 2*(RA18*RA19 - IA18*IA19)*c*d + 2*(RA18*RA20 - IA18*IA20)*c*e + 2*(RA19*RA20 - IA19*IA20)*d*e;

g(5) = (RA21^2 - IA21^2) * a^2 + (RA22^2 - IA22^2) * b^2 + (RA23^2 - IA23^2) * c^2 + (RA24^2 - IA24^2) * d^2 + (RA25^2 - IA25^2) * e^2 + 2*(RA21*RA22 - IA21*IA22)*a*b
 + 2*(RA21*RA23 - IA21*IA23)*a*c + 2*(RA21*RA24 - IA21*IA24)*a*d + 2*(RA21*RA25 - IA21*IA25)*a*e + 2*(RA22*RA23 - IA22*IA23)*b*c + 2*(RA22*RA24 - IA22*IA24)*b*d
 + 2*(RA22*RA25 - IA22*IA25)*b*e + 2*(RA23*RA24 - IA23*IA24)*c*d + 2*(RA23*RA25 - IA23*IA25)*c*e + 2*(RA24*RA25 - IA24*IA25)*d*e;

S = solve(sqrt(g(1))==sqrt(gainmag(1)), sqrt(g(2))==sqrt(gainmag(2)), sqrt(g(3))==sqrt(gainmag(3)), sqrt(g(4))==sqrt(gainmag(4)), sqrt(g(5))==sqrt(gainmag(5)));

for num = 1:length(S.a)
    solution(num,:) = double([S.a(num) S.b(num) S.c(num)]);
    figure(num);
    [gain, deg] = gain1d(dis,solution(num,:),400);
    dbz(deg,gain, 30, 40, 1.5);
end
```

arrayfactor function

```
function AF = arrayfactor(phi,d,n)
AF = exp(j * 2 * n * pi * d * cos(phi));
```

bwidth Function

```
function dphi = bwidth(d, ph0, dpsi)

if nargin==0, help bwidth; return; end

ph0 = ph0 * pi / 180;

if abs(sin(ph0)) < eps,
   dphi = sqrt(2*dpsi / (pi*d));                % endfire
else
   dphi = dpsi / (2 * pi * d * sin(ph0));       % broadside
end

dphi = dphi * 180 / pi;
```

dbz Function

```
function h = dbz(phi, g, rays, Rm, width)

if nargin==0, help dbz; return; end
if nargin<3, rays = 30; end
if nargin<4, Rm = 40; end
if nargin<5, width = 1; end

sty = ':';                                          % grid line style

gdb = g .* (g > eps) + eps * (g <= eps);            % make g=0 into g=eps, avoids -Inf's
gdb = 10 * log10(gdb);
gdb = gdb .* (gdb > -Rm) + (-Rm) * (gdb <= -Rm);    % lowest is Rm dB
gdb = (gdb + Rm)/Rm;                                % scale to unity max.

x = gdb .* cos(phi);
y = gdb .* sin(phi);

N0 = 400;
phi0 = (0:N0) * 2*pi / N0;
x0 = sin(phi0);                                     % gain circles
y0 = cos(phi0);

h = plot(x, y, 'LineWidth', width);
hold on;
plot(x, -y, 'LineWidth', width);                    % -phi part added
hold on;
plot(x0, y0, 0.75*x0, 0.75*y0, sty, 0.50*x0, 0.50*y0, sty, 0.25*x0, 0.25*y0, sty);

axis square;
R = 1.1;
axis([-R, R, -R, R]);
axis off;

Nf = 15;                % fontsize of labels

line([0,0],[-1,1]);
line([-1,1],[0,0]);
```

```
text(0, 1.02,  ' 90^o',   'fontsize', Nf, 'horiz', 'center', 'vert', 'bottom');
text(0, -0.99, '-90^o', 'fontsize', Nf, 'horiz', 'center', 'vert', 'top');

text(1, 0.01,  ' 0^o', 'fontsize', Nf, 'horiz', 'left', 'vert', 'middle');
text(-1.02, 0.01, '180^o',  'fontsize', Nf, 'horiz', 'right', 'vert', 'middle');

text(1.07*cos(pi/12), 1.07*sin(pi/12),  '#phi', 'fontsize', Nf+2, 'horiz', 'left');

if rays == 45,
  x1 = 1/sqrt(2); y1 = 1/sqrt(2);
  line([-x1,x1], [-y1,y1], 'linestyle', sty);
  line([-x1,x1], [y1,-y1], 'linestyle', sty);

  text(1.04*x1, y1,        '45^o',  'fontsize', Nf, 'horiz', 'left', 'vert', 'bottom');
  text(0.97*x1, -0.97*y1,  '-45^o', 'fontsize', Nf, 'horiz', 'left', 'vert', 'top');
  text(-0.97*x1, 1.02*y1,  '135^o',  'fontsize', Nf, 'horiz', 'right', 'vert', 'bottom');
  text(-1.01*x1, -1.01*y1, '-135^o', 'fontsize', Nf, 'horiz', 'right', 'vert', 'top');
else
  x1 = cos(pi/3); y1 = sin(pi/3);
  x2 = cos(pi/6); y2 = sin(pi/6);
  line([-x1,x1], [-y1,y1], 'linestyle', sty);
  line([-x2,x2], [-y2,y2], 'linestyle', sty);
  line([-x2,x2], [y2,-y2], 'linestyle', sty);
  line([-x1,x1], [y1,-y1], 'linestyle', sty);

  text(1.02*x1,1.02*y1,         '60^o',  'fontsize', Nf, 'horiz', 'left', 'vert', 'bottom');
  text(0.95*x1,-0.97*y1,        '-60^o', 'fontsize', Nf, 'horiz', 'left', 'vert', 'top');
  text(1.04*x2,0.97*y2, '30^o', 'fontsize', Nf, 'horiz', 'left', 'vert', 'bottom');
  text(0.98*x2,-0.93*y2,        '-30^o', 'fontsize', Nf, 'horiz', 'left', 'vert', 'top');

  text(-0.91*x1,1.02*y1,  '120^o',  'fontsize', Nf, 'horiz', 'right', 'vert', 'bottom');
  text(-0.97*x1,-1.01*y1, '-120^o', 'fontsize', Nf, 'horiz', 'right', 'vert', 'top');
  text(-1.02*x2,0.97*y2,  '150^o',  'fontsize', Nf, 'horiz', 'right', 'vert', 'bottom');
  text(-1.01*x2,-1.01*y2, '-150^o', 'fontsize', Nf, 'horiz', 'right', 'vert', 'top');
end

s1 = sprintf('-%d', 0.25*Rm);
s2 = sprintf('-%d', 0.50*Rm);
s3 = sprintf('-%d', 0.75*Rm);
```

```
text(0.765, 0.125, s1, 'fontsize', Nf, 'horiz', 'left', 'vert', 'top');
text(0.515, 0.125, s2, 'fontsize', Nf, 'horiz', 'left', 'vert', 'top');
text(0.265, 0.125, s3, 'fontsize', Nf, 'horiz', 'left', 'vert', 'top');

text(0.55, -0.005, 'dB', 'fontsize', Nf, 'horiz', 'left', 'vert', 'top');
```

dtft Function

```
function X = dtft(x, w)

if nargin==0, help dtft; return; end

x = x(:).';                     % make x a row w/o conjugation
w = w(:)';                      % make w a row

L = length(x);

z = exp(-j*w);                  % unit-circle points

X = 0;                          % evaluate z-transform using H"orner's rule
for n = L-1:-1:0,
    X = x(n+1) + z .* X;
end
```

gain1d Function

```
function [g, phi] = gain1d(d, a, N)

if nargin==0, help gain1d; return; end

phi = (0 : N) * pi / N;     % equally-spaced over [0,pi]

psi = 2 * pi * d * cos(phi);

A = dtft(a, -psi);              % array factor, note dsft(a,psi)=dtft(a,-psi)
g = abs(A).^2;                  % power gain
g = g/max(g);                   % normalized to unity maximum
```